Mathematical programming formulations for robust airside terminal traffic flow optimisation problem

Kam K.H. Ng, Chun-Hsien Chen, C.K.M. Lee

Full text available at:
https://www.sciencedirect.com/science/article/abs/pii/S0360835221000231

Doi:
https://doi.org/10.1016/j.cie.2021.107119

APA reference:
Ng, K. K. H., Chen, C.-H., & Lee, C. K. M. (2021). Mathematical programming formulations for robust airside terminal traffic flow optimisation problem. *Computers & Industrial Engineering*, 107119. doi: https://doi.org/10.1016/j.cie.2021.107119.

IEEE reference:
[1] K. K. H. Ng, C.-H. Chen, and C. K. M. Lee, "Mathematical programming formulations for robust airside terminal traffic flow optimisation problem," *Comput Ind Eng*, p. 107119, 2021/01/14/ 2021, doi: https://doi.org/10.1016/j.cie.2021.107119.

Mathematical programming formulations for robust airside terminal traffic flow optimisation problem

Kam K.H. NG [a], Chun-Hsien CHEN [b,*], C.K.M. LEE [c]

[a] *Interdisciplinary Division of Aeronautical and Aviation Engineering, The Hong Kong Polytechnic University, Hong Kong SAR, China*

[b] *School of Mechanical and Aerospace Engineering, Nanyang Technological University, 50 Nanyang Avenue, Singapore 639798, Singapore*

[c] *Department of Industrial and Systems Engineering, The Hong Kong Polytechnic University, Hung Hom, Hong Kong, China*

* *Corresponding author.*

Address: School of Mechanical and Aerospace Engineering, Nanyang Technological University, North Spine, N3.2-B1-02c, 50 Nanyang Avenue, Singapore 637460, Singapore. Tel.: +65 8311 8226

Email Address: kam.kh.ng@polyu.edu.hk (Kam K.H. NG), mchchen@ntu.edu.sg (C.-H. CHEN), ckm.lee@polyu.edu.hk (C.K.M. LEE)

Acknowledgment

The authors would like to express their gratitude and appreciation to the anonymous reviewers, the editor-in-chief and the editorial members for providing valuable comments for the continuing improvement of this article. The research is supported by *Interdisciplinary Division of Aeronautical and Aviation Engineering, The Hong Kong Polytechnic University, Hong Kong SAR, School of Mechanical and Aerospace Engineering, Nanyang Technological University*, Singapore and *Department of Industrial and Systems Engineering*, *The Hong Kong Polytechnic University*, Hong Kong SAR. Our gratitude is also extended to the Research Committee and the *Interdisciplinary Division of Aeronautical and Aviation Engineering, The Hong Kong Polytechnic University* for support of the project (BE3V) and *Department of Industrial and Systems Engineering, The Hong Kong Polytechnic University* for support of the project (RU8H). The authors would like to express their appreciation to *the Hong Kong International Airport* and *FlightGlobal* for their assistance with the data collection.

Declarations of interest: The authors declare that they have no known competing financial interests or personal relationships that could have appeared to influence the work reported in this paper.

Mathematical programming formulations for robust airside terminal traffic flow optimisation problem

Abstract

The robust traffic flow modelling approach offers a perspicacious and holistic surveillance for flight activities in a nearby terminal manoeuvring area. The real time flight information expedites the streaming control of terminal operations using computational intelligence. Hence, in order to reduce the adverse effect of severe uncertainty and the impact of delay propagation, the amplified disruption along with the terminal traffic flow network can be leveraged by using robust optimisation. The transit time from entry waypoint to actual landing time is uncertain since the true airspeed is affected by the wind direction and hazardous aviation weather in the terminal manoeuvring area. Robust optimisation for TTFP is to generate a solution against the uncertain outcomes, which implies that less effort by the ATC to perform re-scheduling is required. In addition, two decomposition methods are presented and proposed in this work. The computational performance of traditional Benders Decomposition will largely be affected by the infeasibility in the subsystem and resolution of infeasible solution in the second-stage optimisation problem resulting in a long iterative process. Therefore, we presented an enhanced Benders Decomposition method to tackle the infeasibility in the subsystem. As shown in the numerical experiments, the proposed method outperforms the traditional Benders Decomposition algorithm using Wilcoxon-signed ranks test and achieved a 58.52% improvement of solution quality in terms of solving one-hour flight traffic scenarios with an hour computation time limit.

Keywords: decomposition methods, robust optimisation, min-max approach, airside terminal traffic flow problem

1. Introduction

Terminal Traffic Flow Problem (TTFP) considers a schedule to determine the approach path selection, approach route, number of aeronautical holding and the landing time in the Terminal Manoeuvring Area (TMA). Adverse weather conditions may induce air traffic delay and Air Traffic Control (ATC) needs to take care all the actions of approaching flights and ensure smooth traffic in the TMA (Wee et al., 2018). Solving the TTFP is complex as various decision required to be made and the performance of a schedule is subjected to the current air traffic situation and traffic control regulation (Ng et al., 2017a). The increased number of passengers and airlines induces the volume of air transportation (Eltoukhy et al., 2017; Lee et al., 2018; Ng et al., 2018). The air route network is far more complex than as more air routes and runway facilities have been introduced (Francis et al., 2004; Gelhausen et al., 2013; Lee et al., 2019). This is also the major issues that most of the international airports have experiences heavy air traffic delay and rescheduling issue in the past two decades (Farhadi et al., 2014; Ng et al., 2015; Wu & Law, 2019). Furthermore, the efficiency of ATC is also subjected to the operational manners and adverse weather condition (Samà et al., 2015, 2017b). The exogenous uncertainty may reduce the air route capacity and contribute to the delay of flight arrival and departure time (Ng et al., 2017a; Wee et al., 2019). We, therefore, believed that the consideration of uncertainty in TTFP is necessary to help ATC to design a smooth approaching ATC schedule (Ng & Lee, 2017; Samà et al., 2017a; Samà et al., 2017b).

The approaching time is not deterministic as the current weather condition and route traffic situation are not accurately predicted (Campanelli et al., 2016; Kafle & Zou, 2016; Pyrgiotis et al., 2013). Terminal traffic flow capacity deficiencies may increase the possibility of delay propagation and flight delay in subsequent ATC activities (Samà et al., 2017a; Samà et al., 2017b). Ng et al. (2017a) suggested that robust optimisation for TTFP can accommodate the effect of aggregate delays and the effect of uncertain parameters in a schedule to achieve high level of solution robustness. Other than the considerations of uncertainty parameters in ATC, resolving potential conflict and collision-free approach route solution should be considered in the model (Qian et al., 2017). An efficient air transportation system must satisfy the needs of smooth airport operations, manageable ATC and utilisation of air routes and runway resources (Gillen et al., 2016).

Most of the literature only considered the runway properties, including runway resources, runway assignment. sequencing problem and safety requirement, in the mathematical model, namely Aircraft Sequencing and Scheduling Problem (ASSP) (Guépet et al., 2017; Herrema et al., 2019; Ng et al., 2018). Air Landing Problem (ALP) and Air Take-off Problem (ATP) are the special runway setting of ASSP (Ng & Lee, 2016a, 2016b; Ng et al., 2017a). Recent research suggested that the final approach operations are affected by the manner of ATC (Hansen & Zou, 2013; Zou & Hansen, 2012). Therefore, it is important to consider the approach route selection, aeronautical decision and air route operations in the decision making (Samà et al., 2017b). The simple model of TTFP is formulated by no-wait job shop scheduling and proposed by Bianco et al. (1997). Samà et al. (2014) presented an alternative graph approach to formulate the TTFP. However, the variables and parameters in the abovementioned models are in deterministic.

The expected and actual operation time may be affected by the uncertain parameters. Indeed, close monitoring of all flights' activities can resolve the problem of uncertainty in ATC, but a more advanced computational unit is required to re-schedule when the predetermined schedule is be disrupted (Du et al., 2020). The contemporary research suggested that the uncertain parameters took into the consideration of mathematical modelling and the robust optimisation model can yield a solution that is vulnerable to disruption (Liang et al., 2018). Stochastic and robust optimisation are the available methods to resolve the uncertainty model. Stochastic process considered the uncertain parameters as a probability-guarantee distribution from the historical data (Jacquillat & Odoni, 2015a, 2015b; Jacquillat et al., 2016). When only limited information on the uncertain parameters is available, robust optimisation offers a risk-averse approach by interval-based uncertain parameters instead of statistical control of uncertainty distribution of the parameters (Aissi et al., 2009; Gabrel et al., 2014; Hu et al., 2016). Ben-Tal et al. (2010) firstly proposed the soft robust model against the downside performance and the worst-case scenarios. Absolute robustness, robust deviation and relative deviation are well-known robust optimisation methods (Xu et al., 2013). Ng et al. (2017a) proposed a min-max regret approach in hedging the uncertain operational time for mixed-mode parallel runway operations.

The robust solution is developed through satisfying the constraints generated by the realisation of the worst-case scenarios (Li et al., 2019c; Wang et al., 2019; Yang et al., 2020). Using the exact algorithm in solving robust optimisation problem significantly increases the overall computational burden compared to solving deterministic or stochastic models. Given the nature of two-stage optimisation in the min-max and min-max regret approach, approximate algorithms, such as heuristics and meta-heuristics, are applicable. Ng et al. (2017a) proposed an Efficient Artificial Bee Colony (EABC) algorithm to develop a robust ASSP schedule. The efficiency of the computational performance outperforms the Genetic Algorithm (GA) and Hybrid Artificial Bee Colony (HABC) algorithm. Additionally, Liu et al. (2016) proposed quantum Ant Colony Optimisation (ACO) for the path optimisation problem. However, meta-heuristics offer a close-to-optimal solution and do not guarantee a proof-of-optimal condition (Elbeltagi et al., 2005; Ng et al., 2018; Ng et al., 2017b). Alternatively, the Bender's Decomposition (BD) approach for robust optimisation has been well studied (Bodur & Luedtke, 2016; Bruni et al., 2017, 2018; Kergosien et al., 2017). Compared to the Branch-and-Bound (B&B) algorithm, decomposing the model by partitioning the decision variables using the BD algorithm enhances the convergence process (Makui et al., 2016; Martins de Sá et al., 2018; Zarrinpoor et al., 2018). In this connection, the iterative relaxation procedure is considered to solve the two-stage optimisation approach in robust optimisation (Cao et al., 2010). Various enhancement scheme on decomposition algorithms were proposed for robust optimisation in the literature, such as Accelerating BD (Makui et al., 2016; Zarrinpoor et al., 2018), BD algorithm with Combinatorial Benders cuts method (BD algorithm with the CBC method) (Cao et al., 2010), BD with tightened lower bound enhancement (Bruni et al., 2017, 2018), and improved BD (Bodur & Luedtke, 2016).

Robust policy is preferable when uncertainty in TMA is inevitable. As for deterministic model for TTFP, one could argue that reactive scheduling approaches can be performed when latest traffic information is available. This required a superior computational performance to achieve real-time or near-time decision since TTFP is a NP-hard problem (Ng et al., 2018). Furthermore, re-scheduling needs to acquire a close monitoring of all flight activities in the TMA and the latest coordinate of the approach flights (Ng et al., 2020; Ng et al., 2017a). Comparatively, robust optimisation for TTFP inherently optimise the solution over the worst-case scenarios when the model is subjected to the deterministic variability, which indicates that the scheduling for TTFP has less vulnerability to disruption, such as hazardous aviation weather in the TMA, current traffic situation and variability of approach speed (Li et al., 2019a; Li et al., 2019b). Less effort is required by the ATC to perform re-scheduling.

1.1. Contribution of the research

The contributions of this article are outlined below. First, an alternative path method to construct the approach path problem is developed. Instead of using the no-wait job-shop scheduling or the alternative graph method, the TTFP model has limited available approach paths from the origin node (entry waypoint) to the destination node (runway). The proposed model is formulated by using Directed Acyclic Graph (DAG), which is a graph that is directed and has no cycles linking the other edges (Ballestín & Leus, 2009; Bruni et al., 2017). Second, a min-max approach for the robust TTFP is introduced. The robust solution is practical and vulnerable to scheduling disruption. Hence, the imprecision of transit time induced by the minimal disturbance of constant flight speed for approach paths within a TMA is presented. Third and foremost, two decomposition methods to solve the proposed robust model are proposed to solve the two-stage optimisation model since the robust TTFP model cannot be solved directly with the property of nonlinearity. A combinatorial cuts method and an enhancement scheme on the first-stage problem are proposed to guarantee a possible convergence to optimise and increase the computational efficiency and solution quality.

1.2. Organisation of the paper

After describing the general background of the robust TTFP and the state-of-the-art robust optimisation and algorithms, the complete formulation of the deterministic TTFP is presented in **Section 2**. **Section 3** illustrates the cardinality of the uncertainty set and robust model with the decomposition framework for TTFP, while **Section 4** describes two novel algorithmic components using a Bender's decomposition structure. The descriptions of the test instances and computational results are illustrated in **Section 5**. The summary of the research and the concluding remarks are raised in **Section 6**.

2. Problem formulation of the deterministic terminal traffic flow model

The mathematical formulation of the deterministic traffic flow model is presented in this section. The Standard terminal arrival routes (STARs) and aeronautical holding for each flight can be assigned by the ATC under area control jurisdiction. The set of STARs is a set of alternative routes from the entry waypoint of the Terminal Transition Routes (TTR) to the runway(s). The area control jurisdiction of ATC is the area of TMA, started from the terminal airspace sector boundary. The entry waypoint refers to the geographical coordinates on the terminal airspace sector boundary between the Air Traffic Service (ATS) route and navigation route (Ng et al., 2018). Aeronautical holding is sometimes required when there is heavy traffic on terminal air space or particular air route (Ng et al., 2017a). In this work, the model can coordinate the current traffic and aeronautical holding assignment to achieve better operational efficiency and flexibility within the decision horizon.

2.1. Assumption of the model

There are several assumptions of the proposed model. The set of approach paths is assumed to be deterministic in the decision horizon. Any changes of the network structure are not available in the model. Furthermore, any missed approaches, emergency operations and abnormal ATC operations in the decision horizon are neglected in the proposed model. The transportation time between waypoint is assumed to fall into an interval case due to the turbulence of weather conditions and wind resistance. Finally, in the case airport, mono-aeronautical holding is sufficient and the number of holding per racetrack pattern is limited to one.

2.2. A toy alternative paths model for explanation

To understand the design of alternative path approach, the following section presents the major components in the deterministic model for TTFP with graphical representation. The approach paths from entry waypoint $u_{i_1}^s$ to runway $u_{i_1}^e$ for all flights $i_1 \in I$ with a decision horizon are considered in the model. For each flight, ATC determines the best approach path from a set of alternative paths. **Fig. 1** depicts the alternative path approach for TTFP. Flight i_1 enters from entry waypoint 1, while flight i_2 enter from entry waypoint 2. The set of alternative paths for flights i_1 and i_2 are $(o,1,3,6,8,d)$, $(o,1,3,4,6,8,d)$, $(o,1,5,6,8,d)$, $(o,1,5,7,8,d) \in P_{i_1}$ and $(o,2,5,6,8,d)$, $(\mathrm{o},2,5,7,8,\mathrm{d})$, $(\mathrm{o},2,7,8,\mathrm{d}) \in P_{i_2}$ respectively. Nodes 3 and 4 indicates the same waypoint but node 4 is regarded as an artificial node to present the entry waypoint after performing one turn of aeronautical holding.

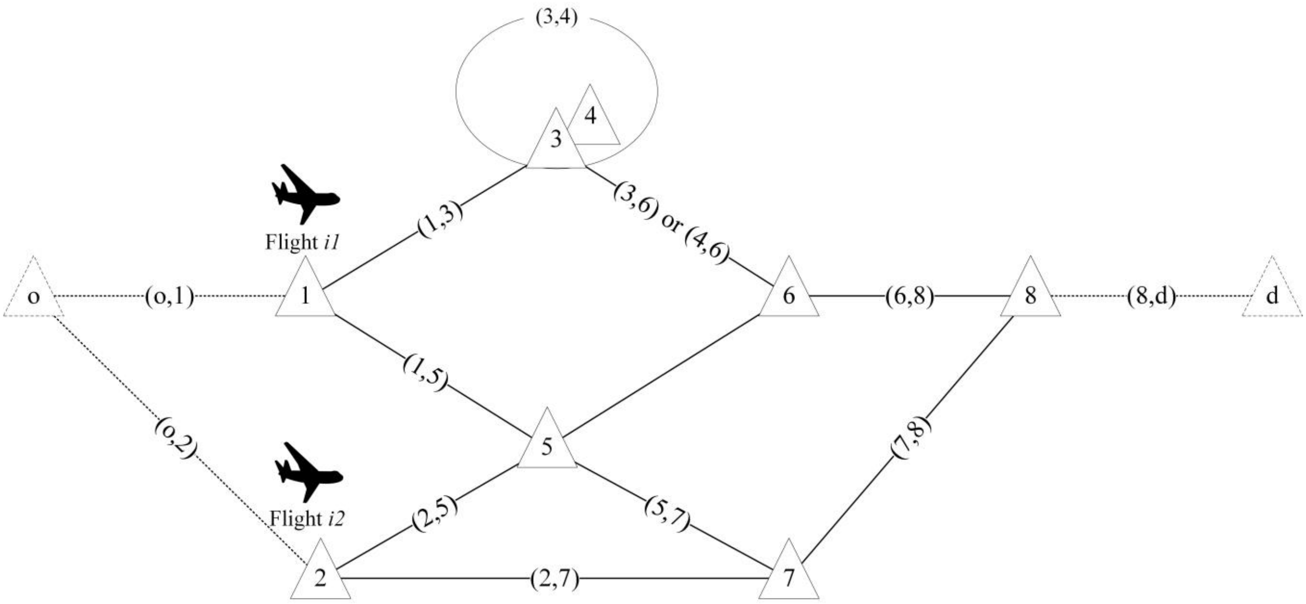

Fig. 1. A schematic diagram of the alternative paths approach for TTFP

Conflict resolution between flights is a method to avoid potential conflict on shared air route resources and to ensure stable approaches for all incoming flights. Path coordination and aeronautical holding are the two common approaches for conflict resolution.

We presume that the longitudinal separation is insufficient and that there is a potential conflict on waypoint 6 if flight i_1 considers $(o,1,3,6,8,d) \in P_{i_1}$, while flight i_2 choose $(o,2,5,6,8,d) \in P_{i_2}$ for approach in **Fig. 2**. In such a case, the path coordination method adopts the conflict detection on each node and determines a feasible solution by coordinating the path planning and choosing the valid paths for both flights i_1 and i_2. Conflict can be resolved by using re-routing strategy for flight j from $(o,2,5,6,8,d) \in P_{i_2}$ to $(o,2,7,8,d) \in P_{i_2}$. Paths with a dotted line indicate a path planning with conflict at waypoint 6, while paths with a solid line demonstrate a valid path planning by considering path coordination as shown in **Fig. 2**.

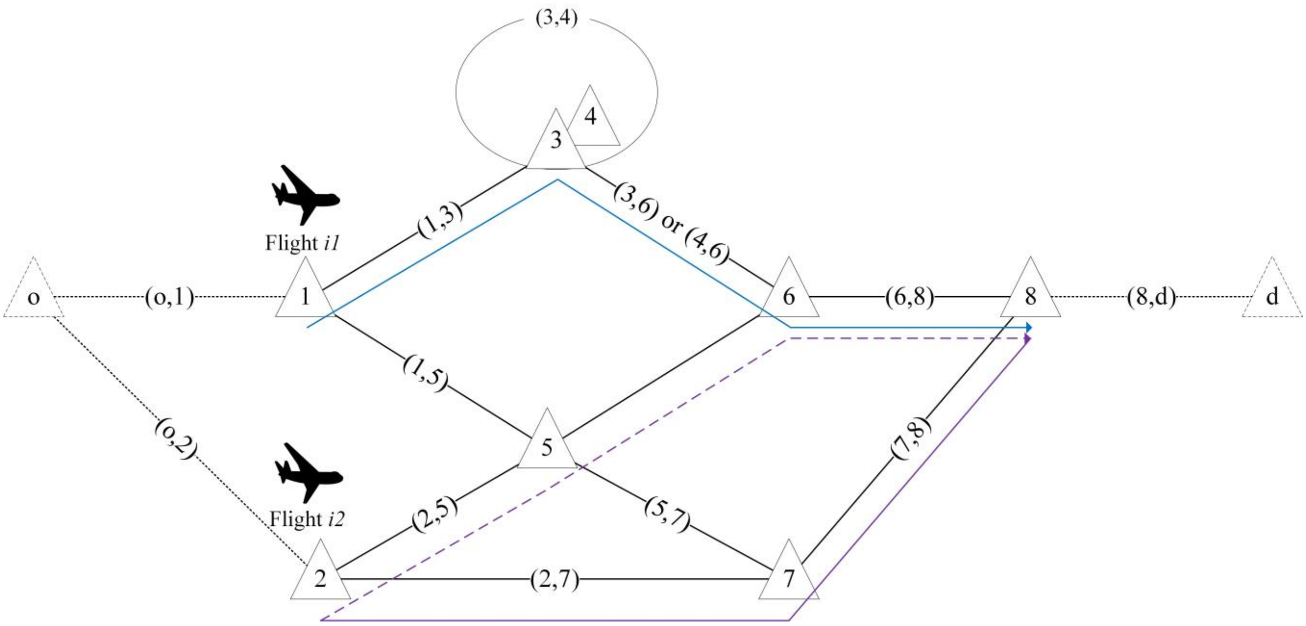

Fig. 2. A schematic diagram of conflict resolution by path coordination

The path coordination approach may not be feasible, since air routes are fixed and resources are limited. Aeronautical holding attempts to impose a delay on an aircraft by keeping it on hold in a racetrack pattern in order to impose a delay adjustment program and to minimise the overall delay in the ATC system. **Fig. 3** presents a schematic diagram of a mono-aeronautical holding approach. A mono-aeronautical holding is represented by a recursive arc on the same node. An artificial node 4 is introduced to distinguish paths with aeronautical holding $(o,1,3,4,6,8,d) \in P_{i_1}$ or without aeronautical holding $(o,1,3,6,8,d) \in P_{i_1}$Given a same scenario that both flights have potential conflict on waypoint 6, flight i may perform mono-aeronautical holding on waypoint 3 by using $(o,1,3,4,6,8,d) \in P_{i_1}$ to impose the delay program on the actual arrival time on waypoints 6 and 8.

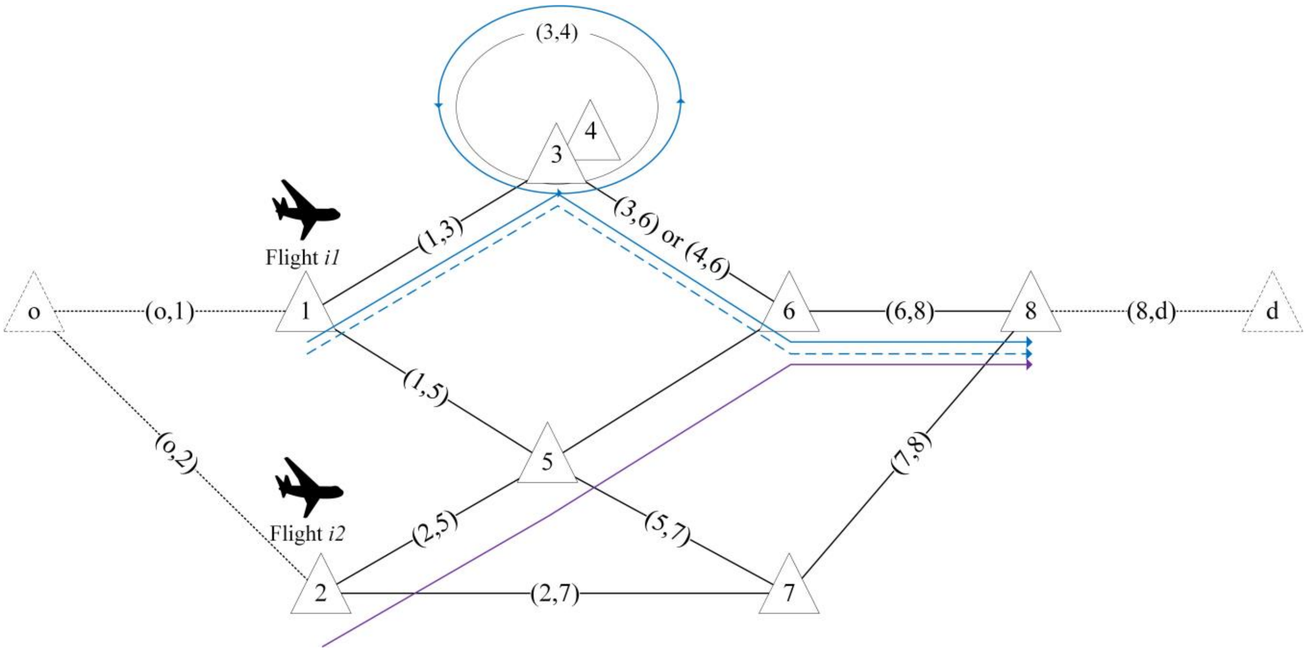

Fig. 3. A schematic diagram of the mono-aeronautical holding

2.3. The deterministic terminal traffic flow model

The TTFP model consists of a set of waypoints V and a set of air route E as a directed graph $G = (V, E)$. In the decision horizon, the model determines the optimal approach path $p_{i_1} = (o, u_{i_1}^s, \dots, u_{i_1}^e, d)$ from a set of alternative paths P_{i_1} for each flight $i_1, i_2, i_3 \in I$. The set of alternative paths P_{i_1} is deterministic. Waypoints o and d are the dummy nodes in the TTFP model. The entry waypoint $u_{i_1}^s$ is subjected to the departed airport and air route network. The destination waypoint $u_{i_1}^e$ is the runway. The air route is any valid pair of waypoints and $(u, v) \in E$ indicate the connection of the directed graph. The set of waypoints of a path is $V_{i_1}^{p_{i_1}}$. Therefore, the collection of all valid waypoint from a set of alternative paths can be represented by $V_{i_1}^{p_{i_1}} \subset V$. Intuitively, the set of air route of a pair is $E_{i_1}^{p_{i_1}} \subset E$. In this connection, $V_{i_1}, V_{i_2} \in V, E_{i_1}, E_{i_2} \in E$ in digraph G. For more detail of the design and description of the deterministic model, readers are referred to Ng et al. (2020).

A solution X is constructed by $\varphi_{i_1}^{p_{i_1}}$ and $z_{i_1 i_2 u}$. The decision variable $\varphi_{i_1}^{p_{i_1}}$ is used to determine the selection of an approach path $p_{i_1} \in P_{i_1}$ for each flight $i_1 \in I$, while $z_{i_1 i_2 u}$denotes the sequential relationship of flights i_1 and i_2 on waypoint u if both flights will pass through the same waypoint. The arrival time at each node u is presented by a continuous decision variable $\tau_{i_1 u}^{p_{i_1}}$, which is associated with selected path p_{i_1} and its corresponding transit waypoint $u \in V_{i_1}^{p_{i_1}}$. The weight coefficient associated with the path selection $w_{i_1}^{p_{i_1}}$ indicates the preference of path selection. $w_{i_1}^{p_{i_1}}$ is equal to the maximum number of holdings along the path. In this regard, zero aeronautical holding would be preferable in path selection when there is a conflict of longitudinal separation. The completion time C indicates the time at which all flights arrive at the runway in the model for TTFP. The notations and decision variables are presented in **錯誤! 書籤的自我參照不正確。**. The deterministic TTFP model is mixed-integer linear programming (MILP) and NP-hard problem (Ng et al., 2020).

Table 1

Notations and decision variables.

Notations	Explanation
i_1, i_2, i_3	Flight ID $i_1, i_2, i_3 \in I$
u, v, π	Transit waypoint $u, v, \pi \in V$
$u_{i_1}^s$	The entry waypoint for flight i_1, $u_{i_1}^s \in V$
$u_{i_1}^e$	The approaching runway for flight i_1, $u_{i_1}^e \in V$
o	Dummy variable of origin node $o \in V$
d	Dummy variable of destination node $d \in V$
ET_{i_1}	Estimated time of arrival at the terminal airspace sector boundary
$w_{i_1}^{p_{i_1}}$	The weight coefficient associated with the path selection $p_{i_1} \in P_{i_1}$
M	Large artificial variable
$t_{i_1(u,v)}$	The mean travel time from nodes u to v for flight i_1
$\tilde{t}_{i_1(u,v)}$	The interval of the travel time from nodes u to v for flight i_1, $\tilde{t}_{i_1(u,v)} = [\underline{t}_{i_1(u,v)}, \overline{t}_{i_1(u,v)}]$, where $\overline{t}_{i_1(u,v)} = \underline{t}_{i_1(u,v)} + \hat{t}_{i_1(u,v)}$
$\delta_{i_1 i_2}$	Separation time on air route between flight i_1 and i_2
Decision variables	**Explanation**
X	A solution X is constructed by $\varphi_{i_1}^{p_{i_1}}$ and $z_{i_1 i_2 u}$
$\varphi_{i_1}^{p_{i_1}}$	1, if flight i_1 is assigned to the path p_{i_1}; 0, otherwise
$z_{i_1 i_2 u}$	1, if flight i_1 is before flight i_2 on node u (not necessary immediately); 0, otherwise
$\tau_{i_1 u}^{p_{i_1}}$	The arrival time on node u using path p_{i_1} for flight $i, \tau_{i_1 u}^{p_{i_1}} \geq 0$
C	The completion time of the terminal traffic flow model

The complete deterministic model is shown as follows:

$$F(X) = \min \sum_{i_1 \in I} \sum_{p_{i_1} \in P_{i_1}} w_{i_1}^{p_{i_1}} \varphi_{i_1}^{p_{i_1}} + C \tag{1}$$

$$s.t.$$

$$\sum_{p_{i_1} \in P_{i_1}} \varphi_{i_1}^{p_{i_1}} = 1, \forall i_1 \in I \tag{2}$$

$$z_{i_1 i_2 u} + z_{i_2 i_1 u} \leq 1, \forall i_1, i_2 \in I, i_1 < i_2, \forall u \in V_{i_2} \cap V_{i_1} \tag{3}$$

$$\varphi_{i_1}^{p_{i_1}} + \varphi_{i_2}^{p_{i_2}} \leq z_{i_2 i_1 u} + z_{i_1 i_2 u} + 1, \forall i_1, i_2 \in I, i_1 \neq i_2, \forall u \in V_{i_2} \cap V_{i_1}, \forall p_{i_1} \in P_{i_1}, \forall p_{i_2} \in P_{i_2} \tag{4}$$

$$z_{i_1 i_3 u} \geq z_{i_1 i_2 u} + z_{i_2 i_3 u} - 1, \forall i_1, i_2, i_3 \in I, i_1 \neq i_2 \neq i_3, \forall u \in V_{i_1} \cap V_{i_2} \cap V_{i_3} \tag{5}$$

$$\tau_{i_1 o}^{p_{i_1}} \geq ET_{i_1} \varphi_{i_1}^{p_{i_1}}, \forall i_1 \in I, \forall p_{i_1} \in P_{i_1} \tag{6}$$

$$\tau_{i_1 u}^{p_{i_1}} \leq M \varphi_{i_1}^{p_{i_1}}, \forall i_1 \in I, \forall u \in P_{i_1} \tag{7}$$

$$C \geq \tau_{i_1 d}^{p_{i_1}}, \forall i_1 \in I, \forall p_{i_1} \in P_{i_1} \tag{8}$$

$$\tau_{i_1 v}^{p_{i_1}} - \tau_{i_1 u}^{p_{i_1}} \geq t_{i_1(u,v)} - \mathrm{M}\left(1 - \varphi_{i_1}^{p_{i_1}}\right), \forall i_1 \in I, p_{i_1} \in P_{i_1}, \forall (u,v) \in E_{i_1}, u < v \tag{9}$$

$$\sum_{\substack{p_i \in P_i \\ u \in V_i^p}} \tau_{iu}^{p_i} - \sum_{\substack{p_j \in P_j \\ u \in V_j^p}} \tau_{ju}^{p_j} \geq \delta_{ji} - M\left(1 - z_{jiu}\right), \forall i, j, \in I, i \neq j, \forall u \in V_j \cap V_i \setminus \{o, d\} \tag{10}$$

$$\varphi_{i_1}^{p_{i_1}} \in \{0,1\}, \forall i_1 \in I, \forall p_{i_1} \in P_{i_1} \tag{11}$$

$$z_{i_1 i_2 u} \in \{0,1\}, \forall i_1, i_2 \in I, i_1 \neq i_2, \forall u \in V_{i_1} \cap V_{i_2} \tag{12}$$

$$\tau_{i_1 u}^{p_{i_1}} \in \mathbb{R}^+, \forall i_1 \in I, \forall p_{i_1} \in P_{i_1}, \forall o, u, d \in P_{i_1} \tag{13}$$

The model is designed as a minimisation problem of weighted path assignment and completion time with an Objective function (1). Constraint set (2) enforces that each flight can only select one path from a set of alternate paths. Constraint set (3) computes the sequence at node u using the binary variable $z_{i_1 i_2 u}$. Constraint set (4) confirms the sequential relationship of flights i_1 and i_2 at node u, where node u must be a complementary element of V_{i_1} and V_{i_2}, while Constraint set (5) explains triangular inequality for flights i_1, i_2 and i_3. The arrival time at the entry waypoint is equal to the time ETA_{i_1} when flight i_1 first appears in the TMA by Constraint set (6). $\tau_{i_1 u}^{p_{i_1}}$ is a non-zero number when path p_{i_1} is selected by Constraint set (7) using the decision variable $\varphi_{i_1}^{p_{i_1}}$. Constraint set (8) computes the completion time, where C indicates the completion time of the schedule. Constraint set (9) ensures the respect of travelling time for flight i_1 from waypoints u to v. Constraint set (10) is the air route longitudinal separation and conflict-free requirements. Constraints (11) and (12) indicate that $\varphi_{i_1}^{p_{i_1}}$ and $z_{i_1 i_2 u}$ are binary variables, while $\tau_{i_1 u}^{p_{i_1}}$ denotes a positive real number by Constraint set (13).

3. The decomposition framework of the robust terminal traffic flow model

In this section, a robust TTFP considers the transit time uncertainty raised by the slight perturbation of cruise speed. The transit time in an air route within a TMA usually falls into an interval case as the travel time of all flights is subject to the variability of actual cruise speed and assigned speed, dynamic weather situation and air route traffic. To reduce the vulnerability to scheduling disruption, a robust criterion is introduced to increase the resilience level of traffic flow scheduling. The robust criterion is a conservative approach in hedging uncertainty and protecting the uncertainty against the worst-case scenarios.

3.1. The cardinality of the uncertainty set

The robust TTFP model attempts to undertake the consideration of travel time uncertainty between waypoints while, at the same time, minimising the completion time of the schedule. In this model, the transit time $\tilde{t}_{i_1(u,v)}$ falls into an interval $\tilde{t}_{i_1(u,v)} = \{\underline{t}_{i_1(u,v)}, \overline{t}_{i_1(u,v)}\}$ to represent the discrepancy of estimated and actual transit times on approach track using Equation (14). $\underline{t}_{i_1(u,v)}$ is denoted as the lower bound of transit time, while $\overline{t}_{i_1(u,v)}$ indicates the upper bound of transit time. $\hat{t}_{i_1(u,v)}$ indicates the deviation between $\underline{t}_{i_1(u,v)}$ and $\overline{t}_{i_1(u,v)}$. In this connection, $\overline{t}_{i_1(u,v)} = \underline{t}_{i_1(u,v)} + \hat{t}_{i_1(u,v)}$. The lower bound of the transit time between waypoints equals to the actual air route distance divided by the economics speed of an aircraft, which is presented in Section 5.1. It is unlikely that the estimated transit time is equal to the actual travel time in operations, as an uncertain travel time between waypoints is subject to minimal perturbation of constant flight speed, weather conditions, wind resistance and the level of scheduling resilience. The variance of transit time will be discussed in more detail in **Section 5.1**. The robust TTFP model is presented in a two-stage optimisation framework.

$$\Phi = \left\{\tilde{t}_{i_1(u,v)}, \forall i_1 \in I, \forall (u,v) \in E_{i_1} \middle| \tilde{t}_{i_1(u,v)} = \underline{t}_{i_1(u,v)} + \hat{t}_{i_1(u,v)} \theta_{i_1(u,v)} \middle| \theta_{i_1(u,v)} \in \{0,1\}\right\} \tag{14}$$

3.2. The robust terminal traffic flow model under travel time uncertainty

As one of the main contributions of this research, we next present the decomposition framework for robust TTFP. The robust TTFP comprises the first-stage optimisation problem to handle the path assignment and approaching sequence using the alternative path approach and the second-stage optimisation problem to compute the travel time and completion time of a schedule. When an uncertainty set of transit time is considered, the model is convex but non-linear, which cannot be directly solved with B&B or B&C solvers. Therefore, a decomposition framework is suggested with the incorporation of optimality cutting plate method in order to solve the model using MILP solver. The objective function (1) of the robust TTFP model under transit time uncertainty is revised in **section 3.2.1**. The completion time of the schedule under worst-case scenario is defined in **section 3.2.2**. In this section, we emphasise the approach deriving the dual form of the second-stage optimisation problem and generating corresponding cuts to the first-stage optimisation problem.

3.2.1. The first-stage optimisation problem

In a general decomposition framework, the recursive approach is to produce a solution from the first-stage optimisation problem and design appropriate cuts by solving the second-stage optimisation problem. The first-stage optimisation problem produces a feasible solution by considering the binary and integer variables to reduce solution time. In the deterministic TTFP model, the decision variables $\varphi_{i_1}^{p_{i_1}}$ and $z_{i_1 i_2 u}$ construct the solution. The formulation of the first-stage optimisation problem is shown as follows:

$$f(X) = \min \sum_{i_1 \in I} \sum_{p_{i_1} \in P_{i_1}} w_{i_1}^{p_{i_1}} \varphi_{i_1}^{p_{i_1}} + d(\boldsymbol{\varphi}, \boldsymbol{z}) \tag{15}$$

,where $d(\boldsymbol{\varphi}, \boldsymbol{z})$ is the completion time of the schedule under worst-case scenario.

$s.t.$

(2) – (5) and (11) – (12)

3.2.2. The second-stage optimisation problem

Dividing the original problem into two outer and inner optimisation problem, the robust counterpart via duality becomes tractable (Bertsimas et al., 2013; Mulvey et al., 1995; Siddiqui et al., 2011). The solution obtained from the first-stage optimisation problem will feed into the second-stage optimisation problem. The optimal solution of the second-stage optimisation problem is determined by the parameterisation of the $\boldsymbol{\varphi}, \boldsymbol{z}$. Given a fixed value of the integer value $\hat{\varphi}$ and $\hat{z}$ from the master problem, a primal second-stage optimisation problem is obtained. The primal second-stage optimisation problem is an independent model with an objective function of the minimisation of the completion time of a schedule over the uncertain set Φ. By introducing the uncertain parameter $\tilde{t}_{i_1 uv}$ as stated in **Section 3.1**, the primal second-stage optimisation problem seeks to maximise the uncertain travel time $\tilde{t}_{i_1 uv}$ between waypoints and minimise the completion time of a schedule by fixing $\boldsymbol{\varphi}, \boldsymbol{z}$.

$$d(\boldsymbol{\varphi}, \boldsymbol{z}) = \min_{\tau} \max_{t \in \Phi} C \tag{16}$$

$s.t.$

(6) – (8), (10) and (13)

$$\tau_{i_1 v}^{p_{i_1}} - \tau_{i_1 u}^{p_{i_1}} \geq \tilde{t}_{i_1 (u,v)} - \mathrm{M}\left(1 - \varphi_{i_1}^{p_{i_1}}\right), \forall i_1 \in I, \forall p_{i_1} \in P_{i_1}, \forall (u,v) \in E_{i_1}, u < v, \forall t \in \Phi \tag{17}$$

The primal second-stage optimisation problem is intractable as the model consists of min-max operators in the objective function. By utilising the dual information, solving the robust TTFP is computationally achievable under a few assumptions of robust optimisation. First, generating the constraints from the second-stage optimisation problem and developing a cutting method can further strengthen the convergence of the first-stage optimisation problem. Second, the dual subproblem is a normalisation strategy to linearly transform the model from a min-max problem to a max-max problem. The dual form of the second-stage optimisation problem can be obtained by introducing the dual variables $a_{i_1}^{p_{i_1}}$, $b_{i_1}^{p_{i_1}}$, $q_{i_1u}^{p_{i_1}}$, $g_{i_1(u,v)}^{p_{i_1}}$ and $h_{i_1i_2u}$ to the Constraints (6), (7), (8), (10) and (17). The dual form of the second-stage optimisation problem is yielded from the primal form of the second-stage optimisation problem using dual theory. Particularly, the dual variable $g_{i_1(u,v)}^{p_{i_1}}$ is a binary variable, with the special dual transformation taking place when the matrix of $g_{i_1(u,v)}^{p_{i_1}}$ is a unimodular matrix, which is a special case in the network flow model (Ford Jr & Fulkerson, 2015; Montemanni & Gambardella, 2005). The matrix is a unimodular matrix when the determinant of every square of the submatrices satisfies the condition of $-1, 0$ or 1. The complete formulation of the dual second-stage optimisation problem by the Equations (18) – (28) is presented as follows:

$$d(\boldsymbol{\varphi},\boldsymbol{z}) = \max_{a,b,q,g,h} \max_{\theta} \sum_{i_1\in I} \sum_{p_{i_1}\in P_{i_1}} \left(ET_{i_1}^{HCI}\hat{\varphi}_{i_1}^{p_{i_1}}\right) b_{i_1}^{p_{i_1}} + \sum_{i_1\in I} \sum_{p_{i_1}\in P_{i_1}} \sum_{u\in V_{i_1}} \left(M\hat{\varphi}_{i_1}^{p_{i_1}}\right) q_{i_1u}^{p_{i_1}} \tag{18}$$

$$+\sum_{i_1\in I} \sum_{p_{i_1}\in P_{i_1}} \sum_{(u,v)\in E_{i_1}} \left(\underline{t}_{i_1(u,v)} + \hat{t}_{i_1(u,v)}\theta_{i_1(u,v)}^{p_{i_1}} - M\left(1-\hat{\varphi}_{i_1}^{p_{i_1}}\right)\right) g_{i_1(u,v)}^{p_{i_1}}$$

$$+\sum_{i_2\in I} \sum_{i_1,i_2\neq i_1\in I} \sum_{u\in V_{i_1}\cap V_{i_2}\setminus\{o,d\}} (S_{i_2i_1} - M(1-\hat{z}_{i_2i_1u}))h_{i_2i_1u}$$

$$s.t.$$

$$\sum_{i_1\in I} \sum_{p_{i_1}\in P_{i_1}} a_{i_1}^{p_{i_1}} \leq 1 \tag{19}$$

$$b_{i_1}^{p_{i_1}} + q_{i_1o}^{p_{i_1}} - g_{i_1(o,u_{i_1}^s)}^{p_{i_1}} - \sum_{i_2,i_1\neq i_2\in I} h_{i_1i_2o} + \sum_{i_1,i_1\neq i_2\in I} h_{i_2i_1o} \leq 0, \forall i_1\in I, \forall p_{i_1}\in P_{i_1}, \forall (\mathrm{o},u_{i_1}^s)\in E_{i_1} \tag{20}$$

$$-a_{i_1}^{p_{i_1}} + q_{i_1d}^{p_{i_1}} + g_{i_1(u_{i_1}^e,d)}^{p_{i_1}} - \sum_{i_2,i_1\neq i_2\in I} h_{i_1i_2d} + \sum_{i_2,i_1\neq i_2\in I} h_{i_2i_1d} \leq 0, \forall i_1\in I, \forall p_{i_1}\in P_{i_1}, \forall (u_{i_1}^e,d)\in E_{i_1} \tag{21}$$

$$q_{i_1v}^{p_{i_1}} + g_{i_1(u,v)}^{p_{i_1}} - g_{i_1(v,\pi)}^{p_{i_1}} - \sum_{\substack{i_2,i_1\neq i_2\in I\\ v\in V_{i_2}\cap V_{i_1}\setminus\{o,d\}}} h_{i_1i_2v} + \sum_{\substack{i_2,i_1\neq i_1\in I\\ v\in V_{i_1}\cap V_{i_2}\setminus\{o,d\}}} h_{i_2i_1v} \leq 0, \forall i_1\in I, \forall p_{i_1}\in P_{i_1}, \tag{22}$$

$$\forall (u,v),(v,\pi)\in E_{i_1}, u<v, v<\pi \setminus \{o,d\}$$

$$a_{i_1}^{p_{i_1}} \in R^+, \forall i_1\in I \tag{23}$$

$$b_{i_1}^{p_{i_1}} \in R^+, \forall i_1\in I, \forall p_{i_1}\in P_{i_1} \tag{24}$$

$$q_{i_1u}^{p_{i_1}} \in R^-, \forall i_1\in I, \forall p_{i_1}\in P_{i_1}, \forall u\in V_{i_1} \tag{25}$$

$$g_{i_1(u,v)}^{p_{i_1}} \in \{0,1\}, \forall i_1\in I, \forall p_{i_1}\in P_{i_1}, \forall (u,v)\in E_{i_1}, u<v \tag{26}$$

$$h_{i_2i_1u} \in R^+, \forall i_1,i_2\in I, i_1\neq i_2, \forall u\in V_{i_1}\cap V_{i_2}\setminus\{o,d\} \tag{27}$$

$$\theta_{i_1(u,v)}^{p_{i_1}} \in \{0,1\}, \forall i_1 \in I, \forall p_{i_1} \in P_{i_1}, \forall (u,v) \in E_{i_1}, u < v \tag{28}$$

The robust optimisation computes the robust solution by realising the uncertain parameters as either an upper bound or lower bound value in worst case optimisation and optimising the objective function. The dual variable $\theta_{i_1(u,v)}^{p_{i_1}}$ is associated with the realisation of an interval case of the travel time between waypoints, while the completion time of a schedule in the dual-problem is a joint decision of the dual variables $a_{i_1}^{p_{i_1}}$, $b_{i_1}^{p_{i_1}}$, $q_{i_1 u}^{p_{i_1}}$, $g_{i_1(u,v)}^{p_{i_1}}$ and $h_{i_2 i_1 u}$. The objective function in the dual form is bilinear with the term $\hat{t}_{i_1(u,v)}\theta_{i_1(u,v)}^{p_{i_1}} g_{i_1(u,v)}^{p_{i_1}}$. However, θ and g are disjoint. In this connection, there is an optimal solution at the extreme points of the disjoint polyhedral (Horst & Tuy, 2013; Montemanni & Gambardella, 2005). Denoting $g_{i_1(u,v)}^{p_{i_1}}$ and $\theta_{i_1(u,v)}^{p_{i_1}}$ as binary variables and the nature of the disjoint polyhedral, Constraints (29) – (32) convert the dual form of the second-stage optimisation problem into a linear form as follow:

$$\begin{aligned} d(\boldsymbol{\varphi}, \boldsymbol{z}) = \max_{a,b,q,g,h,\theta} & \sum_{i_1 \in I} \sum_{p_{i_1} \in P_{i_1}} \left(ET_{i_1} \hat{\varphi}_{i_1}^{p_{i_1}}\right) b_{i_1}^{p_{i_1}} + \sum_{i_1 \in I} \sum_{p_{i_1} \in P_{i_1}} \sum_{u \in V_{i_1}} (M \hat{\varphi}_{i_1}^{p_{i_1}}) q_{i_1 u}^{p_{i_1}} \\ & + \sum_{i_1 \in I} \sum_{p_{i_1} \in P_{i_1}} \sum_{(u,v) \in E_{i_1}} \left(\underline{t}_{i_1(u,v)} - M\left(1 - \hat{\varphi}_{i_1}^{p_{i_1}}\right)\right) g_{i_1(u,v)}^{p_{i_1}} \\ & + \sum_{i_1 \in I} \sum_{p_{i_1} \in P_{i_1}} \sum_{(u,v) \in E_{i_1}} (\hat{t}_{i_1(u,v)}) w_{i_1(u,v)}^{p_{i_1}} \\ & + \sum_{i_2 \in I} \sum_{i_1, i_1 \neq i_2 \in I} \sum_{u \in V_{i_1} \cap V_{i_2} \setminus \{o,d\}} (S_{i_2 i_1} - M(1 - \hat{z}_{i_2 i_1 u})) h_{i_2 i_1 u} \end{aligned} \tag{29}$$

$s.t.$

$$w_{i_1(u,v)}^{p_{i_1}} \leq \theta_{i_1(u,v)}^{p_{i_1}}, \forall i_1 \in I, \forall p_{i_1} \in P_{i_1}, \forall (u,v) \in E_{i_1}, u < v \tag{30}$$

$$w_{i_1(u,v)}^{p_{i_1}} \leq g_{i_1(u,v)}^{p_{i_1}}, \forall i_1 \in I, \forall p_{i_1} \in P_{i_1}, \forall (u,v) \in E_{i_1}, u < v \tag{31}$$

$$w_{i_1(u,v)}^{p_{i_1}} \geq 0, \forall i_1 \in I, \forall p_{i_1} \in P_{i_1}, \forall (u,v) \in E_{i_1}, u < v \tag{32}$$

(19) – (28)

4. Illustrations of the decomposition methods

Decomposition framework for solving certain large-scale combinatorial optimisation problem by partitioning the decision variables into complicating variables y and non-complicating variables x (Benders, 1962). Benders (1962) explained that solving large-scale combinatorial optimisation problems is time-consuming. The general idea of benders decomposition is to fix the non-complicating variables x (usually binary and integer variables) and solve the model with the complicating variables y (usually continuous variables) (Bagger et al., 2018).

The decomposition framework for robust TTFP is presented in **Section 3.2**. However, due to a weak connection of the feasible region between the first-stage and second-stage optimisation problem, the iterative process of the framework may enter into a deadlock. To be more specific, a valid cut must be generated at each iteration to reduce the search region and continue the progress towards an optimal solution. Therefore, one well-known cutting scheme and one proposed enhancement strategy are developed in **Sections 4.1** and **4.2**, respectively. The combinatorial cuts method is able to tackle the situation when the solution from the subproblem is infeasible. However, Saharidis and Ierapetritou (2010) argues that the convergence of the decomposition algorithm is slow as combinatorial cuts method is regarded as no good cuts. In order to improve the convergence, additional restrictions and additional constraints on the first-stage optimisation problem could lead to a fast convergence process. Therefore, to avoid the generation of the Minimum Infeasible Subsystems (MISs) cut, we propose an enhancement scheme for the master problem.

4.1. Combinatorial cuts method

In the general decomposition framework, the infeasibility of second-stage optimisation problem implies that the original problem is unbounded or the feasible region of the primal problem is empty (Cao et al., 2010; de Sá et al., 2013; Li et al., 2018). Nonetheless, the robust model does not benefit from the general Benders cut, as the solution produced by the first-stage optimisation problem is not necessarily feasible in the second-stage optimisation problem. Given the special structure of the robust model for TTFP, the general Benders cut in the TTFP may cause the deadlock situation when no valid cuts was obtained by solving the subproblem in the previous iteration. Hooker (2011) and Fischetti et al. (2010) introduced a cutting plane scheme by MISs to tackle infeasibility in the subproblem. In this section, combinatorial Bender's cuts are presented. This algorithm is denoted as BD algorithm with the CBC method.

4.1.1. Benders optimality cut

When the second-stage optimisation problem is solved, a Benders optimality cut is generated and will be added to the formulation of the first-stage optimisation problem. By solving the dual form of the subproblem, the optimal dual variables can be retrieved at the ζth iteration by Equation (33). The completion time of a schedule C must satisfy the dual information at the ζth iteration. Using the Benders dual method, the optimality cut at the ζth iteration can be obtained by Equation (34),while Equation (35) illustrates the feasibility cut at the ζth iteration when subproblem is unbounded.

$$C = \sum_{i_1 \in I} \sum_{p_{i_1} \in P_{i_1}} \left(ET_{i_1} \hat{\varphi}_{i_1}^{p_{i_1}}\right) b_{i_1}^{p_{i_1}\zeta} + \sum_{i_1 \in I} \sum_{p_{i_1} \in P_{i_1}} \sum_{u \in V_{i_1}} \left(M \hat{\varphi}_{i_1}^{p_{i_1}}\right) q_{i_1 u}^{p_{i_1}\zeta}$$
$$+ \sum_{i_1 \in I} \sum_{p_{i_1} \in P_{i_1}} \sum_{(u,v) \in E_{i_1}} \left(\underline{t}_{i_1(u,v)} - M\left(1 - \hat{\varphi}_{i_1}^{p_{i_1}}\right)\right) g_{i_1(u,v)}^{p_{i_1}\zeta}$$
$$+ \sum_{i_1 \in I} \sum_{p_{i_1} \in P_{i_1}} \sum_{(u,v) \in E_{i_1}} (\hat{t}_{i_1(u,v)}) w_{i_1(u,v)}^{p_{i_1}\zeta} + \sum_{i_1 \in I} \sum_{i_2, i_1 \neq i_2 \in I} \sum_{u \in V_{i_1} \cap V_{i_2} \backslash \{o,d\}} \left(S_{i_2 i_1} - M\left(1 - \hat{z}_{i_2 i_1 u}\right)\right) h_{i_2 i_1 u}^{\zeta} \tag{33}$$

$$C \geq \sum_{i_1 \in I} \sum_{p_{i_1} \in P_{i_1}} \left(ET_{i_1} \varphi_{i_1}^{p_{i_1}}\right) \hat{b}_{i_1}^{p_{i_1}\zeta} + \sum_{i_1 \in I} \sum_{p_{i_1} \in P_{i_1}} \sum_{u \in V_{i_1}} \left(M \varphi_{i_1}^{p_{i_1}}\right) \hat{q}_{i_1 u}^{p_{i_1}\zeta}$$
$$+ \sum_{i_1 \in I} \sum_{p_{i_1} \in P_{i_1}} \sum_{(u,v) \in E_{i_1}} \left(\underline{t}_{i_1(u,v)} - M\left(1 - \varphi_{i_1}^{p_{i_1}}\right)\right) \hat{g}_{i_1(u,v)}^{p_{i_1}\zeta}$$
$$+ \sum_{i_1 \in I} \sum_{p_{i_1} \in P_{i_1}} \sum_{(u,v) \in E_{i_1}} (\hat{t}_{i_1(u,v)}) \theta_{i_1(u,v)}^{p_{i_1}} \hat{g}_{i_1(u,v)}^{p_{i_1}\zeta} + \sum_{i_1 \in I} \sum_{i_2, i_1 \neq i_2 \in I} \sum_{u \in V_{i_1} \cap V_{i_1 2} \backslash \{o,d\}} \left(S_{i_2 i_1} - M\left(1 - z_{i_2 i_1 u}\right)\right) \hat{h}_{i_2 i_1 u}^{\zeta} \tag{34}$$

$$0 \geq \sum \sum \left(ET_{i_1} \varphi_{i_1}^{p_{i_1}}\right) \hat{b}_{i_1}^{p_{i_1}\zeta} + \sum \sum \sum \left(M \varphi_{i_1}^{p_{i_1}}\right) \hat{q}_{i_1 u}^{p_{i_1}\zeta} \tag{35}$$

$$+\sum_{i_1\in I}\sum_{p_{i_1}\in P_i}\sum_{(u,v)\in E_{i_1}}\left(\hat{t}_{i_1(u,v)}\right)\theta_{i_1(u,v)}^{p_{i_1}}\hat{g}_{i_1(u,v)}^{p_{i_1}\zeta}+\sum_{i_1\in I}\sum_{i_2,i_2\neq i_1\in I}\sum_{u\in V_{i_1}\cap V_{i_2}\setminus\{o,d\}}\left(S_{i_2 i_1}-M\left(1-z_{i_2 i_1 u}\right)\right)\hat{h}_{i_2 i_1 u}^{\zeta}$$

4.1.2. Minimal infeasible subsystems

The rationale for developing a cut using MISs from the subproblem is to avoid a deadlock when the subproblem is infeasible during the convergence process. If the linear system is infeasible, the cut generated by the MISs enforces the subsystem to change at least one binary variable(s) $\boldsymbol{\varphi}$ and $\boldsymbol{z}$ breaking the infeasibility. The MISs cut will further restrict the solution space of the master problem using Equation (36).

$$\sum_{i_1\in I}\sum_{p_{i_1}\in P_{i_1}|\varphi_{i_1}^{p_{i_1}\xi}=0}\varphi_{i_1}^{p_{i_1}}+\sum_{i_1\in I}\sum_{i_2,i_1\neq i_2\in I}\sum_{u\in V_{i_1}\cap V_{i_2}\setminus\{o,d\}|z_{i_2 i_1 u}^{\xi}=0} z_{i_2 i_1 u}+\sum_{i_1\in I}\sum_{p_{i_1}\in P_{i_1}|\varphi_{i_1}^{p_{i_1}\xi}=1}\left(1-\varphi_{i_1}^{p_{i_1}}\right)$$
$$+\sum_{i_1\in I}\sum_{i_2,i_1\neq i_2\in I}\sum_{u\in V_{i_1}\cap V_{i_2}\setminus\{o,d\}|z_{i_2 i_1 u}^{\xi}=1}\left(1-z_{i_2 i_1 u}\right)\geq 1 \tag{36}$$

4.1.3. Combinatorial Benders cuts method

The BD with CBC method is derived from the Benders dual and MISs methods (Hooker, 2011). In this connection, The Benders cuts by Equations (38) and (39) and the MISs cut $\xi\in\Pi$ from the infeasible region by Equation (40) can be enumerated. The complete first-stage optimisation problem is shown as follows. **Table 2** presents the pseudo code of the CBC algorithm.

$$f(X)=\min\sum_{i_1\in I}\sum_{p_{i_1}\in P_{i_1}} w_{i_1}^{p_{i_1}}\varphi_{i_1}^{p_{i_1}}+C \tag{37}$$

$$s.t.$$

(2) – (5) and (11), (12)

$$C\geq\sum_{i_1\in I}\sum_{p_{i_1}\in P_{i_1}}\left(ET_{i_1}\varphi_{i_1}^{p_{i_1}}\right)\hat{b}_{i_1}^{p_{i_1}\zeta}+\sum_{i_1\in I}\sum_{p_{i_1}\in P_{i_1}}\sum_{u\in V_{i_1}}\left(M\varphi_{i_1}^{p_{i_1}}\right)\hat{q}_{i_1 u}^{p_{i_1}\zeta}$$
$$+\sum_{i_1\in I}\sum_{p_{i_1}\in P_{i_1}}\sum_{(u,v)\in E_{i_1}}\left(\underline{t}_{i_1(u,v)}-M\left(1-\varphi_{i_1}^{p_{i_1}}\right)\right)\hat{g}_{i_1(u,v)}^{p_{i_1}\zeta}$$
$$+\sum_{i_1\in I}\sum_{p_{i_1}\in P_{i_1}}\sum_{(u,v)\in E_{i_1}}\left(\hat{t}_{i_1(u,v)}\right)\theta_{i_1(u,v)}^{p_{i_1}}\hat{g}_{i_1(u,v)}^{p_{i_1}\zeta}$$
$$+\sum_{i_1\in I}\sum_{i_2,i_2\neq i_1\in I}\sum_{u\in V_{i_1}\cap V_{i_2}\setminus\{o,d\}}\left(S_{i_2 i_1}-M\left(1-z_{i_2 i_1 u}\right)\right)\hat{h}_{i_2 i_1 u}^{\zeta},\forall\zeta\in\Lambda^{\rho} \tag{38}$$

$$0 \geq \sum_{i_1 \in I} \sum_{p_{i_1} \in P_{i_1}} \left(E_{i_1} \varphi_{i_1}^{p_{i_1}}\right) \hat{b}_{i_1}^{p_{i_1}\zeta} + \sum_{i_1 \in I} \sum_{p_{i_1} \in P_{i_1}} \sum_{u \in V_{i_1}} \left(M \varphi_{i_1}^{p_{i_1}}\right) \hat{q}_{i_1 u}^{p_{i_1}\zeta}$$
$$+ \sum_{i_1 \in I} \sum_{p_{i_1} \in P_{i_1}} \sum_{(u,v) \in E_{i_1}} \left(\underline{t}_{i_1(u,v)} - M\left(1 - \varphi_{i_1}^{p_{i_1}}\right)\right) \hat{g}_{i_1(u,v)}^{p_{i_1}\zeta}$$
$$+ \sum_{i_1 \in I} \sum_{p_{i_1} \in P_{i_1}} \sum_{(u,v) \in E_{i_1}} \left(\hat{t}_{i_1(u,v)}\right) \theta_{i_1(u,v)}^{p_{i_1}} \hat{g}_{i_1(u,v)}^{p_{i_1}\zeta}$$
$$+ \sum_{i_1 \in I} \sum_{i_2, i_1 \neq i_1 \in I} \sum_{u \in V_{i_1} \cap V_{i_2} \backslash \{o,d\}} \left(S_{i_2 i_1} - M\left(1 - z_{i_2 i_1 u}\right)\right) \hat{h}_{i_2 i_1 u}^{\zeta}, \forall \zeta \in \Lambda^{\varrho} \tag{39}$$

$$\sum_{i_1 \in I} \sum_{p_{i_1} \in P_{i_1} | \varphi_{i_1}^{p_{i_1}\xi} = 0} \varphi_{i_1}^{p_{i_1}} + \sum_{i_1 \in I} \sum_{i_2, i_1 \neq i_1 \in I} \sum_{u \in V_{i_1} \cap V_{i_2} \backslash \{o,d\} | z_{i_2 i_1 u}^{\xi} = 0} z_{i_2 i_1 u} + \sum_{i_1 \in I} \sum_{p_{i_1} \in P_{i_1} | \varphi_{i_1}^{p_{i_1}\xi} = 1} \left(1 - \varphi_{i_1}^{p_{i_1}}\right)$$
$$+ \sum_{i_1 \in I} \sum_{i_2, i_1 \neq i_2 \in I} \sum_{u \in V_{i_1} \cap V_{i_2} \backslash \{o,d\} | z_{i_2 i_1 u}^{\xi} = 1} \left(1 - z_{i_2 i_1 u}\right) \geq 1, \forall \xi \in \Pi \tag{40}$$

Table 2

The pseudo code of combinatorial Benders cuts method

Set $UB = \infty, LB = -\infty,\ iter = 0,\ CPU\_limit$
While $Gap \geq ExitGap$ and $CPU_{current} \leq CPU_{limit}$ **do**
Solve first-stage optimisation problem (2) – (5), (11) – (12), (15)
$LB \leftarrow \psi_{MP}(\varphi, z)$
Solve linear form of dual second-stage optimisation problem (29) – (32), (31) – (40)
Add optimality cut (34) to first-stage optimisation problem, if second-stage optimisation problem is feasible
Add feasibility cut (35) to first-stage optimisation problem, if second-stage optimisation problem is unbounded
Add MISs cut (36) to first-stage optimisation problem, if second-stage optimisation problem is infeasible
Update $UB \leftarrow \psi_{sp}(a, b, q, g, h, \theta)$, if necessary
$Gap = (UB - LB)/UB$
$iter = iter + 1$
End

4.2. Enhanced decomposition algorithm

This section presents the enhancement on the first-stage optimisation problem, which is referred as the Enhanced Benders Decomposition (EBD). From the previous section, the infeasibility of the subproblem exists when the first-stage optimisation problem does not the convergence process of the two-stage optimisation framework to be a feasible region. Instead of considering the MISs to tighten the searching from the feasible region, a restriction scheme on the feasibility of $\boldsymbol{\varphi}$ and $\boldsymbol{z}$ in both the two-stage optimisation framework is developed.

4.2.1. Modification on the first-stage optimisation problem

The dual function of the second-stage optimisation problem is to compute the completion time of a schedule and to maximise the uncertain travel time. Comparatively, the extreme point scenario from the first-stage optimisation problem by considering the lower bound scenario of travel time $t_{i_1 uv}^{LB}$ using Equation (41) ensures feasibility in the second-stage optimisation problem. This inequality states that the transit time from waypoints u to v must be larger or equal to the lower bound transit time in the deterministic case. The amended formulation of the first-stage optimisation problem is shown as follows:

(15)

$s.t.$

$$\tau_{i_1 v}^{p_{i_1}} - \tau_{i_1 u}^{p_{i_1}} \geq t_{i_1(u,v)}^{LB} - \mathrm{M}(1 - \varphi_{i_1}^{p_{i_1}}), \forall i_1 \in I, \forall p_{i_1} \in P_{i_1}, \forall (u,v) \in E_{i_1}, u < v \quad (41)$$

(6) – (8) and (10)

The enhancement of the first-stage optimisation problem moderates the computational effort in the second-stage optimisation problem. Only optimality cuts is generated from each iteration. The pseudo code of enhanced Benders decomposition is presented in **Table 3**.

Table 3

The pseudo code of enhanced Benders decomposition

Set $UB = \infty, LB = -\infty,\ iter = 0,\ CPU\_limit$
While $Gap \geq ExitGap$ and $CPU_{current} \leq CPU_{limit}$ **do**
    Solve first-stage optimisation problem (2) – (8), (10) – (12), (15), (41)
    $LB \leftarrow \psi_{MP}(\varphi, z)$
    Solve linear form of dual second-stage optimisation problem (29) – (32), (31) – (40)
    Add optimality cut (34) to first-stage optimisation problem, if second-stage optimisation problem is feasible
    Add feasibility cut (35) to first-stage optimisation problem, if second-stage optimisation problem is unbounded
    Update $UB \leftarrow \psi_{sp}(a, b, q, g, h, \theta)$, if necessary
    $Gap = (UB - LB)/UB$
    $iter = iter + 1$
End

5. Results of experiments

5.1. Description of the test instances

In this paper, one set of instances is considered for the robust TTFP. We aimed at investigating the algorithm performance regarding the computational efficiency with the consideration of variables manipulation. Therefore, a set of random instances generated by discrete distribution is evaluated in the numerical experiments. The set of instances follows the distribution of real data in April 2018 at The Hong Kong International Airport (HKIA). The data was obtained by a licensed Application Programming Interface (API) from *FlightGlobal*. A total of 14,496 arrival records were extracted after clearing the missing values.

In the robust model, we believed that the expected and the actual transit time on approach route are deviated, as the minimal perturbation of the flight speed is subject to the weather performance, wind direction and speed, turbulence and the degree of the system-level fault resilience of the ATC. In practice, the actual speed is not purely constant, even if a flight is assigned a fixed speed on the approach route. Furthermore, in robust optimisation, the robust solution is totally protected by the realisation of the uncertainty set. In this connection, the robust solution guarantees feasibility in actual operation if we are confident that the uncertain parameters are fluctuated within the interval. The following is the general setting of the robust model for TTFP. Equations (42) and (43) explain that the interval of the transit time is determined by the speed variations $\underline{\omega}_{i_1}$ and $\overline{\omega}_{i_1}$, given a fixed transit distance between nodes $\kappa_{(u,v)}$. **Table 4** presents the normal speed profile (knots) regarding the different sizes of the flights. **Table 5** introduces the longitudinal separation (in nautical miles) between adjacent approaching flights.

$$\underline{t}_{i_1(u,v)} = \frac{\kappa_{(u,v)}}{\overline{\omega}_{i_1}}, \forall i_1 \in I, \forall (u,v) \in E_{i_1}, u < v \tag{42}$$

$$\hat{t}_{i_1(u,v)} = \frac{\kappa_{(u,v)}}{\underline{\omega}_{i_1}} - \frac{\kappa_{(u,v)}}{\overline{\omega}_{i_1}}, \forall i_1 \in I, \forall (u,v) \in E_{i_1}, u < v \tag{43}$$

Table 4

Normal speed profile regarding the flight classes

$knots$[a]	LSF	MSF	SSF
$\underline{\omega}_i$	250	250	275
$\overline{\omega}_i$	300	270	295
$\Delta\overline{v}_i$	50	20	20

[a]: $v_i\ knots = 3600\ v_i\ NM/s$, SSF: Small size flight; MSF: Medium size flight; LSF: Large size flight

Table 5

Longitudinal separation distance (in nautical miles)

NM	LSF	MSF	SSF
LSF	4	5	7
MSF	3	3	5
SSF	3	3	3

SSF: small size flight; MSF: medium size flight; LSF: large size flight

Fig. 4 presents the STARs and geographical positions of the holding circles. As the length of the holding pattern is sufficient to tackle the conflict situation of the air route setting at the HKIA, a mono-aeronautical holding pattern is imposed in the setting of the model (Artiouchine et al., 2008). In accordance with the assumption and the instance of the environmental setting, 10 entry waypoints and 26 alternative paths are constructed in our model as shown in **Fig. 5**.

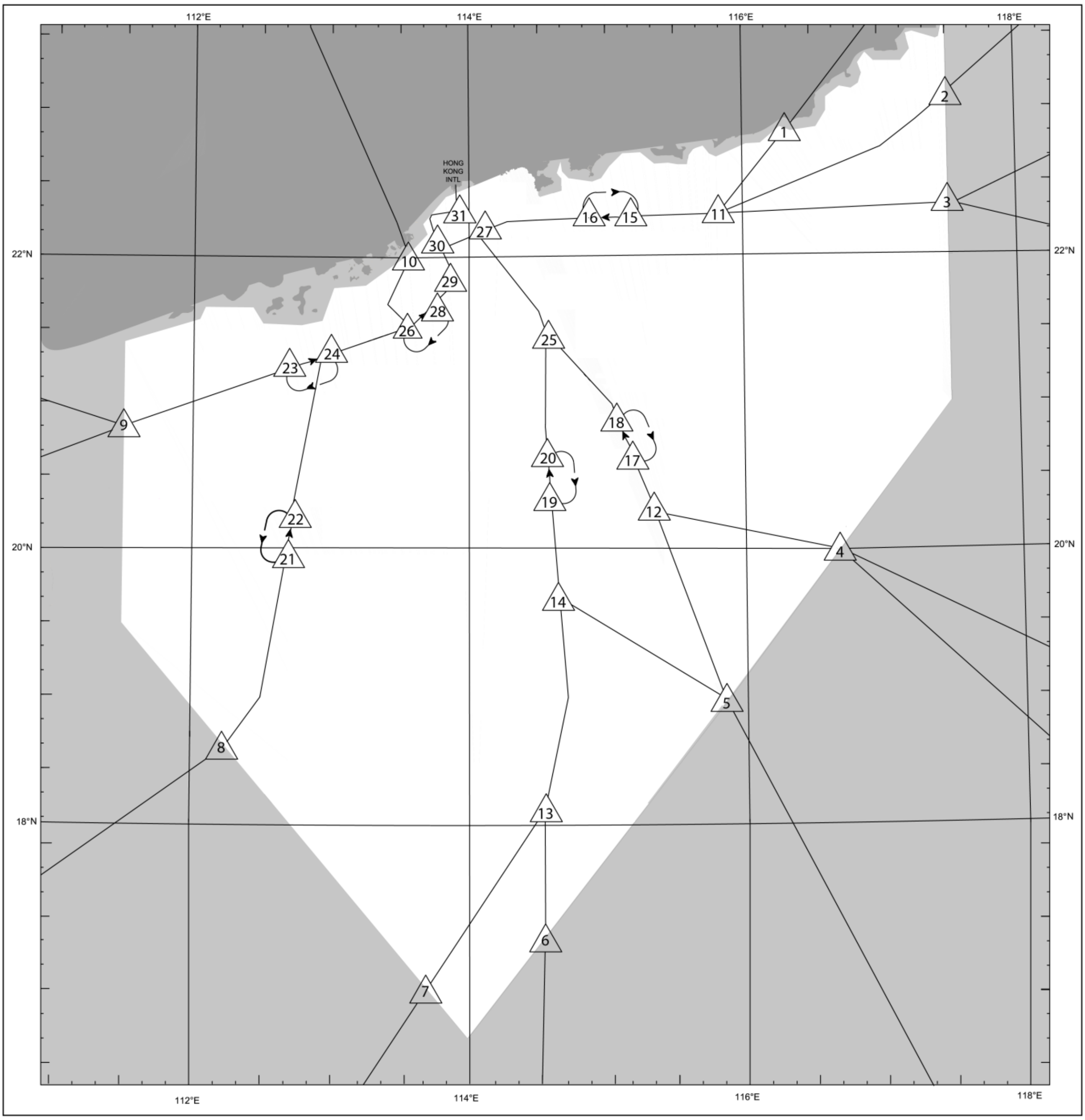

Fig. 4. The air route network in the terminal manoeuvring area

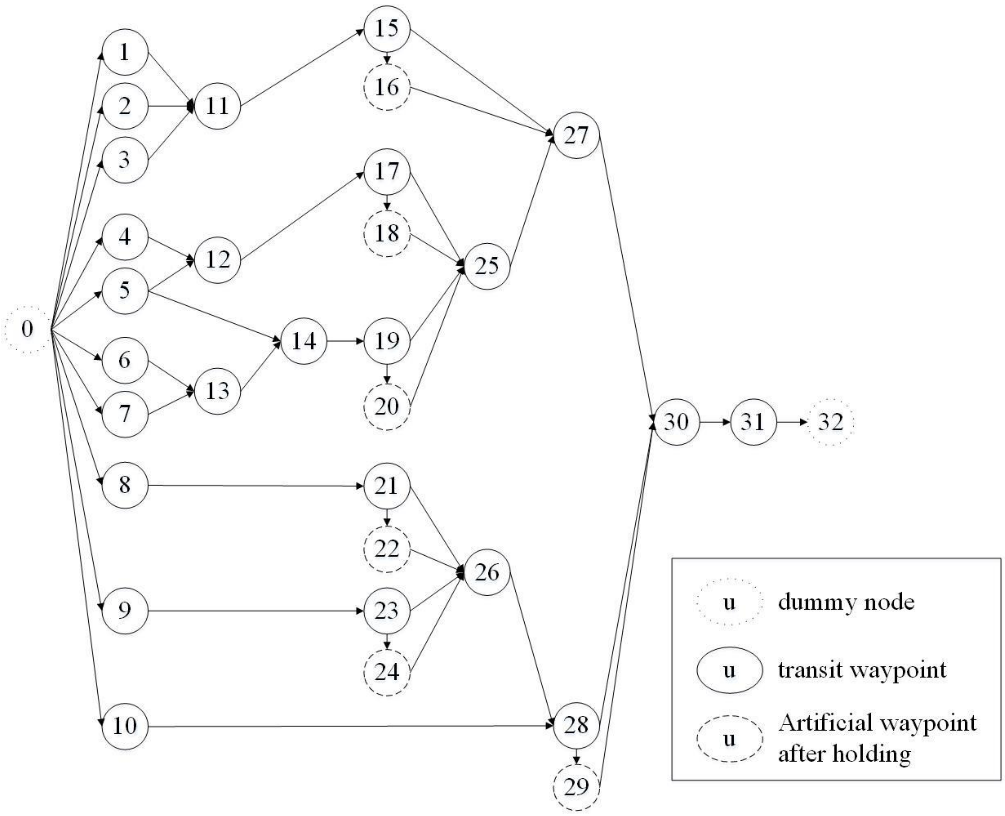

Fig. 5. Digraph representation of the arrival paths with mono-aeronautical holding

The design of the random instances generated by discrete distribution is presented. The characteristics of the testing instances attempt to imitate the patterns found in the real-world scenarios of HKIA in April 2018. **Fig. 6** summarises the average arrival movement at hourly intervals, as the arrival patterns usually depend on the air traffic demand and the preferences of passengers. Normally, heavy traffic occurs during the operating time from 9:00 hours to 22:00 hours, while the normal and light traffic is also indicated in **Fig. 6**. **Table 6** provides the statistical record of the arrival movement using average, standard deviation and minimum and maximum values of the air traffic movement.

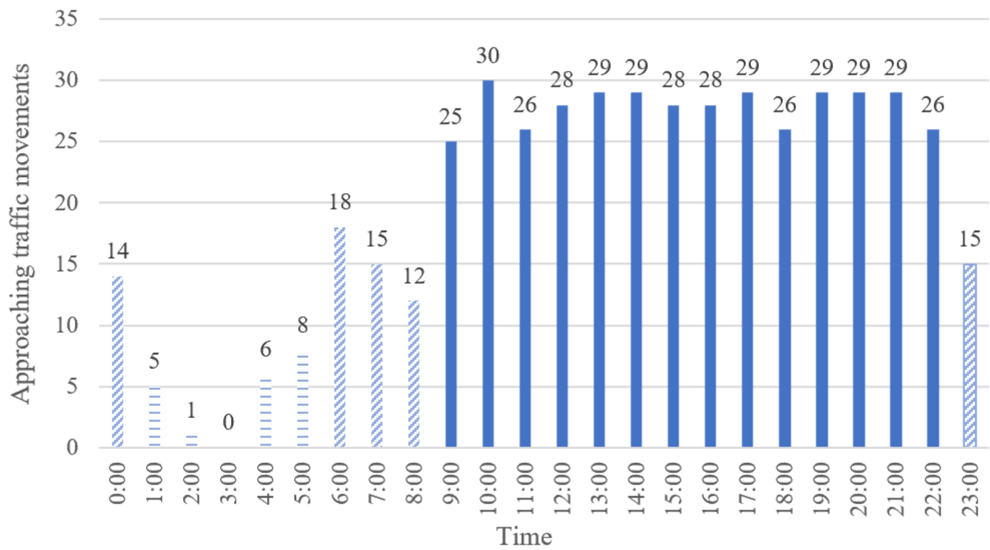

Fig. 6. Average value of the number of flights' approaching traffic movements

Table 6

Statistical summary of the approaching movements in Hong Kong (April 2018)

Traffic class	Approaching movement per hour			
	μ	σ	LB	UB
Heavy	27.9	1.48	24.90	29.87
Normal	14.9	2.10	12.20	17.97
Light	4.07	3.35	0.40	8.04

Heavy traffic problem is usually caused by the overcrowded traffic on the same approach route, constraints on the longitudinal separation and the vortex generated by the aircraft engine. Since our model concerns the air traffic in HKIA scenarios, the generated instances follow the discrete patterns from real-world instances. The discrete distribution of the STARs and aircraft sizes from historical data are analysed as a reference to generate the test instances for numerical experiments. The corresponding distributions are shown in **Table 7** and **Table 8**. For each setting, three instances were generated following the discrete probabilistic distributions. The number of arrival flights for light, normal and heavy traffic were $I = 2, 4, 6, 8$, $I = 12, 14, 16, 18$ and $I = 24, 26, 28, 30$, respectively. A total of 36 test instances were generated.

Table 7

The distribution of standard terminal arrival routes from historical data (April 2018)

STAR		1	2	3	4	5	6	7	8	9	10
Heavy traffic	Frequency	817	862	3831	559	495	151	503	381	1532	2578
	Ratio	6.98%	7.36%	32.72%	4.77%	4.23%	1.29%	4.30%	3.25%	13.08%	22.02%
Normal traffic	Frequency	37	66	632	223	147	41	55	41	385	539
	Ratio	1.71%	3.05%	29.18%	10.30%	6.89%	1.89%	2.54%	1.89%	17.77%	24.88%
Light traffic	Frequency	0	3	176	29	33	45	28	20	82	205
	Ratio	0.00%	0.48%	28.34%	4.67%	5.31%	7.25%	4.51%	3.22%	13.20%	33.10%

STARs: Standard terminal arrival routes

Table 8

The distribution of aircraft sizes from historical data (April 2018)

Flight size		SSF	MSF	LSF
Heavy traffic	Frequency	4245	3202	2552
	Ratio	42.45%	32.02%	25.52%
Normal traffic	Frequency	666	696	804
	Ratio	30.75%	32.13%	37.12%
Light traffic	Frequency	178	175	268
	Ratio	28.66%	28.18%	43.16%

SSF: small size flight; MSF: medium size flight; LSF: large size flight

5.2. Computational analysis

The computation was performed with the configuration of Intel Core I7 3.60GHz CPU and 16 GB RAM under the *Windows 7 Enterprise 64-bit* operating environment. The proposed decomposition algorithms were coded using *C#* language with *Microsoft Visual Studio 2017* and *IBM ILOG CPLEX optimisation Studio 12.8.0*. The value of big M is 10^7.

5.2.1. Measurement

In order to evaluate the algorithm's performance, the optimality gap of the decomposition framework is evaluated in the computational analysis. First, each instance represents a traffic scenario of one hour at the HKIA. Therefore, the computational limit CPU_limit was enforced by 3,600 seconds. The stopping criteria of the two-stage optimisation framework was determined by the gap between UB and LB or the computational time over CPU_limit, which is 3600 seconds. In this connection, the convergence of optimal condition $LB \geq UB$ within the CPU_limit is one of the measurements in the computational analysis. The optimality gap is represented by Equation (44) to indicate the solution quality at the end of the computations. zero value represents an optimal condition, while positive $Optimality\ gap\ \%$ illustrates an approximated or close-to-optimal solution. Second, the convergence rate was analysed.

$$Optimality\ gap\ \%\ (OG\%) = \frac{UB - LB}{UB} \tag{44}$$

5.3. Computational results

With the aim of evaluating the performance of the two proposed algorithms, the computational results present the general findings in accordance with the statistical randomly generated instances. Three traffic scenarios were evaluated with different numbers of flights considered in the system. The computational results by the BD algorithm with the CBC method and EBD algorithm for light, normal and heavy traffic scenarios are presented in **Table 9**, **Table 10** and **Table 11** respectively. Detailed results are presented in **Appendix A** (see **Table 15**, **Table 16** and **Table 17**).

Regarding the solution quality, the EBD algorithm outperforms the BD algorithm with the CBC method. As for light traffic scenarios (see **Table 9**), the BD algorithm with CBC method and EBD algorithms were both able to converge to the global optimal point except for in one instance. As for the instances of normal and heavy traffic scenarios, the solutions of the BD algorithm with the CBC method were not able to converge to the global optimal point within the one-hour computation time. As for the instances with the number of flights being 12, the EBD algorithm could obtain an optimal solution, while for other instances, the EBD algorithm guarantees a close-to-optimal solution (see **Table 10** and **Table 11**).

Table 9

Computational performance for statistical randomly generated instances from light traffic scenarios

Instance		The BD algorithm with CBC method				EBD algorithm			
I	set	UB	LB	$OG\%$	CPU	UB	LB	$OG\%$	CPU
2	a	4951.14	4951.14	**0.00%**	0.18	4951.14	4951.14	**0.00%**	0.17
	b	6739.58	6739.58	**0.00%**	0.03	6739.58	6739.58	**0.00%**	0.09
	c	6370.82	6370.82	**0.00%**	1.51	6370.82	6370.82	**0.00%**	1.83
4	a	6325.82	6325.82	**0.00%**	36.76	6325.82	6325.82	**0.00%**	10.33
	b	8578.31	8578.31	**0.00%**	0.25	8578.31	8578.31	**0.00%**	0.33
	c	8578.31	8578.31	**0.00%**	0.15	8578.31	8578.31	**0.00%**	0.46
6	a	5436.14	5436.14	**0.00%**	2.91	5436.14	5436.14	**0.00%**	1.17
	b	5436.14	5436.14	**0.00%**	3.02	5436.14	5436.14	**0.00%**	1.32
	c	6968.02	6968.02	**0.00%**	2.78	6968.02	6968.02	**0.00%**	25.74
8	a	8094.31	8094.31	**0.00%**	3.99	8094.31	8094.31	**0.00%**	9.92
	b	7721.23	7721.23	**0.00%**	38.59	7721.23	7721.23	**0.00%**	1.56
	c	7061.65	0	100.00%	3600	6704.02	6704.02	**0.00%**	2.44

CPU: computation time in seconds; bold value: best algorithm gap in percentage

Table 10

Computational performance for statistical randomly generated instances from normal traffic scenarios

Instance		The BD algorithm with CBC method				EBD algorithm			
I	set	UB	LB	$OG\%$	CPU	UB	LB	$OG\%$	CPU
12	a	9007.79	0	100.00%	3600	8069.98	8069.98	**0.00%**	40.59
	b	8761.88	0	100.00%	3600	8050.31	8050.31	**0.00%**	9.95
	c	8960.61	0	100.00%	3600	8504.31	8504.31	**0.00%**	3.13
14	a	8971.29	0	100.00%	3600	8260.98	7156.67	**13.37%**	3600
	b	7930.85	0	100.00%	3600	7036.28	6313	**10.28%**	3600
	c	8221.77	0	100.00%	3600	7241.1	5808.67	**19.78%**	3600
16	a	9796	0	100.00%	3600	8252.13	6098.81	**26.09%**	3600
	b	9079.71	0	100.00%	3600	8103.23	7046.67	**13.04%**	3600
	c	8938.41	0	100.00%	3600	7349.24	6444.67	**12.31%**	3600
18	a	9479.68	0	100.00%	3600	8132.23	6528.67	**19.72%**	3600
	b	9425.81	0	100.00%	3600	7545.06	6709.88	**11.07%**	3600
	c	7935.84	0	100.00%	3600	6919.9	5301.32	**23.39%**	3600

CPU: computation time in seconds; bold value: best algorithm gap in percentage

Table 11

Computational performance for statistical randomly generated instances from heavy traffic scenarios

Instance		The BD algorithm with CBC method				EBD algorithm			
I	set	UB	LB	$OG\%$	CPU	UB	LB	$OG\%$	CPU
	a	9854.4	0	100.00%	3600	7496.81	6101.67	**18.61%**	3600
24	b	10314.33	0	100.00%	3600	7933.27	6596.67	**16.85%**	3600
	c	10762.67	0	100.00%	3600	8366.11	6988.87	**16.46%**	3600
	a	11143.12	0	100.00%	3600	9290.61	6390.45	**31.22%**	3600
26	b	11218.62	0	100.00%	3600	8508.47	7317.21	**14.00%**	3600
	c	11575.27	0	100.00%	3600	8519.39	6843.33	**19.67%**	3600
	a	10137.11	0	100.00%	3600	7786.68	6439.24	**17.30%**	3600
28	b	10137.11	0	100.00%	3600	8342.03	7504.33	**10.04%**	3600
	c	11107.23	0	100.00%	3600	7980.74	6496.67	**18.60%**	3600
	a	11100.38	0	100.00%	3600	8668.39	6332.14	**26.95%**	3600
30	b	11100.38	0	100.00%	3600	8828.95	6526.67	**26.08%**	3600
	c	11100.38	0	100.00%	3600	8826.13	6324.67	**28.34%**	3600

CPU: computation time in seconds; bold value: best algorithm gap in percentage

To illustrate the descriptive statistical difference between the BD algorithm with CBC method and the EBD algorithm, the average performance of computation time, average $Optimality\ gap\ \%$ are presented in **Table 12**. The computation time increased along with the complexity of air traffic. As for the instances with normal and heavy traffic, both algorithms could not obtain the optimal solutions. Indeed, the upper bound still decreased along with the computation. However, 100% of Average $OG\%$ represents a condition where no valid Benders cuts were added to tighten the lower bound value in the master problem using the BD algorithm with CBC method. Comparatively, the EBD algorithm obtained valid cuts with the Average $OG\%$ value of 12.42% and 20.4% for instances with normal and heavy traffic respectively, which indicates more valid Benders' cuts using the EBD algorithm. The EBD algorithm yield a 58.52% improvement (69.44% - 10.92%) than the BD algorithm with CBC method. **Table 13** presents the descriptive statistics of the proposed algorithms. The EBD algorithm has low mean value μ and standard deviation σ than the BD algorithm with CBC method.

Table 12

Comparison of the average performance across different traffic scenarios

	BD algorithm with CBC method		EBD algorithm	
	Average CPU	Average $OG\%$	Average CPU	Average $OG\%$
Light traffic	307.51	**8.33%**	4.61	**0.00%**
Normal traffic	3600	**100%**	2704.47	**12.42%**
Heavy traffic	3600	**100%**	3600	**20.40%**
Overall	2502.51	**69.44%**	2103.03	**10.92%**

Table 13

The descriptive statistics of the proposed algorithms with sample size of 36

	μ	σ	Min.	Max.	25th percentiles	50th percentiles	75th percentiles
BD algorithm with CBC method	69.44%	46.72%	0.00%	100.00%	0.00%	100.00%	100.00%
EBD algorithm	10.92%	10.50%	0.00%	31.22%	0.00%	11.69%	19.41%

Wilcoxon-signed ranks test is performed to evaluate the convergence performance ($OG\%$) between the two proposed algorithms through paired sample cases in statistical analysis. This testing is suitable for the two samples which cannot be assumed to be normally distributed. The statistical analysis was conducted with the software *IBM SPSS Statistics 22*. **Table 14** presents the comparison of the convergence performance using Wilcoxon-signed ranks test. The result shows that the paired sample testing obtained a p-value $p \leq 0.001$, which indicate the strength of the effect size is large. We can conclude that the EBD algorithm outperforms the BD algorithm with CBC method.

Table 14

Wilcoxon-signed ranks test between the two proposed algorithms

Algorithms (sample size = 36)	Z score	Asmp. Sig. (2 tailed)	Strength of the effect size
EBD algorithm v.s. BD algorithm with CBC method	-4.374	0.000	Large effect

5.4. Managerial insights

A novel alternative path approach for robust terminal traffic flow problem using a min-max criterion is proposed. Current research still focuses on the reassignment method or ground delay programs to alleviate and partially absorb the effect of disrupted scheduling and passenger unease. We addressed that the transit time from a enter route to the runway is uncertain. The non-stochastic events and exogenous delay may be caused by unanticipated weather disruption, turbulence, wind direction and system-level fault resilience. The propagation of airside delay risk at the terminal area may affect the predetermined scheduling solution and induce the possibility of re-routing. With the introduction of uncertainty parameters in robust optimisation the vulnerability to disruption can further be improved. Fault-driven re-scheduling efforts and aggregate delays can be alleviated and partially absorbed using robust criteria in scheduling. In order to balance the quality of decision making and worst case risk over the uncertainty, Robust schedule for TTFP offers a method to construct a solution with certain level of solution robustness and provide robust decision by considering the ambiguity of underlying distribution of unknown parameters. With the recent advancement of optimisation methods, it can effectively obtain a near optimal with reasonable time of computation for commercial engineering applications. A certain level of solution robustness should not be neglected in ATC operations. The propagation of terminal traffic delays can attribute to the cause of rescheduling and scheduling intervention in daily operation. Robust optimisation is a promising approach that can leverage the delay propagation and guarantee a certain level of solution robustness under the limited knowledge on the distribution of the underlying uncertainty. The delay costs caused by rising air traffic demands includes administration costs for ASSP reassignment, the ripple effect on subsequent flight scheduling, the financial cost of delayed management and passenger dissatisfaction can be reduced.

6. Concluding remarks

This research presents a novel alternative path approach for the robust TTFP under exogenous uncertainty. The uncertainty of the travel time is affected by the unpleasant weather conditions and turbulence in TMA. Therefore, the min-max criterion is suggested in the model. We aim to develop a robust schedule that has less vulnerable to disruption and less effect on the change of predefined schedule. By introducing the uncertain transit time between waypoints in arrival decision management, ATC can obtain a solution that is less sensitivity to disruption of approaching flight time, which imply a less chance on adjusting the approaching schedule in operation.

Regarding the solution produced by the two-stage robust optimisation, in the robust TTFP, the first-stage optimisation problem does not guarantee feasibility in the second-stage optimisation problem. Therefore, two modifications of the decomposition approaches, namely BD algorithm with CBC method and EBD, are proposed. To meet the practical requirements, the computational analysis mainly focused on the efficiency of convergence within reasonable computational limit by the two proposed algorithms. The computational results illustrate that the EBD outperforms the BD with CBC method with the 58.52% improvement of optimality gap on average within an hour computational limit. The Wilcoxon-signed ranks test also empirically proved that there is a significant difference between the optimality gap of EBD algorithm and BD algorithm with CBC method in the numerical experiment. Enumerating all possible worst-case scenarios is time-consuming. However, a closer optimality gap implies a better solution against the uncertainty outcome and disruption. The proposed method can achieve better solution quality than the benchmarking algorithm.

Several future directions can be taken in relation to the proposed model. First, the uncertainty environment in the proposed model is purely conservative. A decision maker may sacrifice a proportion of the robustness of a schedule with less protection, with respect to uncertainty using adjustable robust criteria. Second, the assumption of the terminal traffic flow model can be released in accordance with the structure of a TMA and the airport. For instance, a dynamic change of wind direction will affect the approach route in different time scenarios. Third, an investigation of other computational approaches in robust optimisation methods is of importance to the practical usage in actual ATC. Third, the design of the scheduling in robust optimisation for TTFP may affect the posterior schedule. The integration of rolling horizon and robust optimisation could be combined to obtain a more comprehensive schedule design. Furthermore, adjustable robust optimisation could also be incorporated to amend the posterior ATC schedule when more information regarding the uncertain parameters are available.

Appendices

Appendix A. Detailed computational results for the BD algorithm with CBC method and the EBD algorithm

Table 15

The number of iterations, optimality cuts and MISs cut for statistical randomly generated instances from light traffic scenarios

		The BD algorithm with CBC method					EBD algorithm			
I	set	$OG\%$	$iteration$	$\#\ opt\ cut$	$\#\ fea\ cut$	$\#\ MISs$	$OG\%$	$iteration$	$\#\ opt\ cut$	$\#\ fea\ cut$
2	a	0.00%	3	3	0	0	0.00%	2	2	0
	b	0.00%	3	3	0	0	0.00%	2	2	0
	c	0.00%	16	16	0	0	0.00%	27	27	0
4	a	0.00%	326	325	0	1	0.00%	63	63	0
	b	0.00%	8	8	0	0	0.00%	3	3	0
	c	0.00%	8	8	0	0	0.00%	3	3	0
6	a	0.00%	55	35	0	20	0.00%	7	7	0
	b	0.00%	55	35	0	20	0.00%	7	7	0
	c	0.00%	31	30	0	1	0.00%	91	91	0
8	a	0.00%	37	23	0	14	0.00%	18	18	0
	b	0.00%	238	197	0	41	0.00%	5	5	0
	c	100.00%	4272	4208	0	64	0.00%	4	4	0

$\#\ opt\ cut$: number of optimality cuts; $\#\ fea\ cut$: number of feasibility cuts; $\#\ MISs$: number of cuts generated by MISs

Table 16

The number of iterations, optimality cuts and MISs cut for statistical randomly generated instances from normal traffic scenarios

		The BD algorithm with CBC method					EBD algorithm			
I	set	$OG\%$	$iteration$	$\#\ opt\ cut$	$\#\ fea\ cut$	$\#\ MISs$	$OG\%$	$iteration$	$\#\ opt\ cut$	$\#\ fea\ cut$
12	a	100.00%	4316	4299	0	17	0.00%	11	11	0
	b	100.00%	5506	1810	0	3696	0.00%	5	5	0
	c	100.00%	5782	5781	0	1	0.00%	6	6	0
14	a	100.00%	3575	2481	0	1094	13.37%	910	910	0
	b	100.00%	3386	3385	0	1	10.28%	6823	6823	0
	c	100.00%	4212	577	0	3635	19.78%	1281	1281	0
16	a	100.00%	1350	2	0	1348	26.09%	1533	1533	0
	b	100.00%	2127	2126	0	1	13.04%	1824	1824	0
	c	100.00%	2011	1940	0	71	12.31%	3544	3544	0
18	a	100.00%	854	4	0	850	19.72%	641	641	0
	b	100.00%	762	760	0	2	11.07%	4216	4216	0
	c	100.00%	837	776	0	61	23.39%	1858	1858	0

$\#\ opt\ cut$: number of optimality cuts; $\#\ fea\ cut$: number of feasibility cuts; $\#\ MISs$: number of cuts generated by MISs

Table 17

The number of iterations, optimality cuts and MISs cut for statistical randomly generated instances from heavy traffic scenarios

		The BD algorithm with CBC method					EBD algorithm			
I	set	$OG\%$	$iteration$	$\#\ opt\ cut$	$\#\ fea\ cut$	$\#\ MISs$	$OG\%$	$iteration$	$\#\ opt\ cut$	$\#\ fea\ cut$
24	a	100.00%	78	16	0	62	18.61%	367	367	0
	b	100.00%	91	21	0	70	16.85%	307	307	0
	c	100.00%	91	13	0	78	16.46%	320	320	0
26	a	100.00%	44	1	0	43	31.22%	107	107	0
	b	100.00%	61	2	0	59	14.00%	422	422	0
	c	100.00%	36	2	0	34	19.67%	398	398	0
28	a	100.00%	33	8	0	25	17.30%	883	883	0
	b	100.00%	33	8	0	25	10.04%	1214	1214	0
	c	100.00%	5	2	0	3	18.60%	395	395	0
30	a	100.00%	3	1	0	2	26.95%	128	128	0
	b	100.00%	3	1	0	2	26.08%	141	141	0
	c	100.00%	3	1	0	2	28.34%	71	71	0

$\#\ opt\ cut$: number of optimality cuts; $\#\ MISs$: number of cuts generated by MISs

References

Aissi, H., Bazgan, C., & Vanderpooten, D. (2009). Min–max and min–max regret versions of combinatorial optimization problems: A survey. *European Journal of Operational Research, 197*(2), 427-438. doi:https://doi.org/10.1016/j.ejor.2008.09.012.

Artiouchine, K., Baptiste, P., & Dürr, C. (2008). Runway sequencing with holding patterns. *European Journal of Operational Research, 189*(3), 1254-1266. doi:https://doi.org/10.1016/j.ejor.2006.06.076.

Bagger, N.-C. F., Sørensen, M., & Stidsen, T. R. (2018). Benders' decomposition for curriculum-based course timetabling. *Computers & Operations Research, 91*, 178-189. doi:https://doi.org/10.1016/j.cor.2017.10.009.

Ballestín, F., & Leus, R. (2009). Resource-Constrained Project Scheduling for Timely Project Completion with Stochastic Activity Durations. *Production and Operations Management, 18*(4), 459-474. doi:doi:10.1111/j.1937-5956.2009.01023.x.

Ben-Tal, A., Bertsimas, D., & Brown, D. B. (2010). A soft robust model for optimization under ambiguity. *Operations Research, 58*(4-part-2), 1220-1234.

Benders, J. F. (1962). Partitioning procedures for solving mixed-variables programming problems. *Numerische Mathematik, 4*(1), 238-252. doi:10.1007/bf01386316.

Bertsimas, D., Litvinov, E., Sun, X. A., Zhao, J., & Zheng, T. (2013). Adaptive Robust Optimization for the Security Constrained Unit Commitment Problem. *IEEE Transactions on Power Systems, 28*(1), 52-63. doi:10.1109/TPWRS.2012.2205021.

Bianco, L., Dell'Olmo, P., & Giordani, S. (1997). Scheduling Models and Algorithms for TMA Traffic Management. In L. Bianco, P. Dell'Olmo, & A. R. Odoni (Eds.), *Modelling and Simulation in Air Traffic Management* (pp. 139-167). Berlin, Heidelberg: Springer Berlin Heidelberg.

Bodur, M., & Luedtke, J. R. (2016). Mixed-integer rounding enhanced benders decomposition for multiclass service-system staffing and scheduling with arrival rate uncertainty. *Management Science, 63*(7), 2073-2091.

Bruni, M. E., Di Puglia Pugliese, L., Beraldi, P., & Guerriero, F. (2017). An adjustable robust optimization model for the resource-constrained project scheduling problem with uncertain activity durations. *Omega, 71*, 66-84. doi:https://doi.org/10.1016/j.omega.2016.09.009.

Bruni, M. E., Di Puglia Pugliese, L., Beraldi, P., & Guerriero, F. (2018). A computational study of exact approaches for the adjustable robust resource-constrained project scheduling problem. *Computers & Operations Research, 99*, 178-190. doi:https://doi.org/10.1016/j.cor.2018.06.016.

Campanelli, B., Fleurquin, P., Arranz, A., Etxebarria, I., Ciruelos, C., Eguíluz, V. M., & Ramasco, J. J. (2016). Comparing the modeling of delay propagation in the US and European air traffic networks. *Journal of Air Transport Management, 56*, 12-18. doi:http://dx.doi.org/10.1016/j.jairtraman.2016.03.017.

Cao, J. X., Lee, D.-H., Chen, J. H., & Shi, Q. (2010). The integrated yard truck and yard crane scheduling problem: Benders' decomposition-based methods. *Transportation Research Part E: Logistics and Transportation Review, 46*(3), 344-353. doi:https://doi.org/10.1016/j.tre.2009.08.012.

de Sá, E. M., de Camargo, R. S., & de Miranda, G. (2013). An improved Benders decomposition algorithm for the tree of hubs location problem. *European Journal of Operational Research, 226*(2), 185-202. doi:https://doi.org/10.1016/j.ejor.2012.10.051.

Du, X., Lu, Z., & Wu, D. (2020). An intelligent recognition model for dynamic air traffic decision-making. *Knowledge-Based Systems, 199*, 105274. doi:https://doi.org/10.1016/j.knosys.2019.105274.

Elbeltagi, E., Hegazy, T., & Grierson, D. (2005). Comparison among five evolutionary-based optimization algorithms. *Advanced Engineering Informatics, 19*(1), 43-53. doi:https://doi.org/10.1016/j.aei.2005.01.004.

Eltoukhy, A. E. E., Chan, F. T. S., & Chung, S. H. (2017). Airline schedule planning: a review and future directions. *Industrial Management & Data Systems, 117*(6), 1201-1243. doi:doi:10.1108/IMDS-09-2016-0358.

Farhadi, F., Ghoniem, A., & Al-Salem, M. (2014). Runway capacity management–an empirical study with application to Doha International Airport. *Transportation Research Part E: Logistics and Transportation Review, 68*, 53-63.

Fischetti, M., Salvagnin, D., & Zanette, A. (2010). A note on the selection of Benders' cuts. *Mathematical Programming, 124*(1), 175-182. doi:10.1007/s10107-010-0365-7.

Ford Jr, L. R., & Fulkerson, D. R. (2015). *Flows in networks*: Princeton university press.

Francis, G., Humphreys, I., & Ison, S. (2004). Airports' perspectives on the growth of low-cost airlines and the remodeling of the airport–airline relationship. *Tourism Management, 25*(4), 507-514. doi:http://dx.doi.org/10.1016/S0261-5177(03)00121-3.

Gabrel, V., Murat, C., & Thiele, A. (2014). Recent advances in robust optimization: An overview. *European Journal of Operational Research, 235*(3), 471-483. doi:https://doi.org/10.1016/j.ejor.2013.09.036.

Gelhausen, M. C., Berster, P., & Wilken, D. (2013). Do airport capacity constraints have a serious impact on the future development of air traffic? *Journal of Air Transport Management, 28*, 3-13. doi:http://dx.doi.org/10.1016/j.jairtraman.2012.12.004.

Gillen, D., Jacquillat, A., & Odoni, A. R. (2016). Airport demand management: The operations research and economics perspectives and potential synergies. *Transportation Research Part A: Policy and Practice, 94*, 495-513. doi:https://doi.org/10.1016/j.tra.2016.10.011.

Guépet, J., Briant, O., Gayon, J.-P., & Acuna-Agost, R. (2017). Integration of aircraft ground movements and runway operations. *Transportation Research Part E: Logistics and Transportation Review, 104*, 131-149. doi:https://doi.org/10.1016/j.tre.2017.05.002.

Hansen, M., & Zou, B. (2013). Airport Operational Performance and Its Impact on Airline Cost. In *Modelling and Managing Airport Performance* (pp. 119-143): John Wiley & Sons.

Herrema, F., Curran, R., Hartjes, S., Ellejmi, M., Bancroft, S., & Schultz, M. (2019). A machine learning model to predict runway exit at Vienna airport. *Transportation Research Part E: Logistics and Transportation Review, 131*, 329-342. doi:https://doi.org/10.1016/j.tre.2019.10.002.

Hooker, J. (2011). *Logic-based methods for optimization: combining optimization and constraint satisfaction* (Vol. 2): John Wiley & Sons.

Horst, R., & Tuy, H. (2013). *Global optimization: Deterministic approaches*: Springer Science & Business Media.

Hu, H., Ng, K. K. H., & Qin, Y. (2016). Robust Parallel Machine Scheduling Problem with Uncertainties and Sequence-Dependent Setup Time. *Scientific Programming, 2016*, 13. doi:10.1155/2016/5127253.

Jacquillat, A., & Odoni, A. R. (2015a). Endogenous control of service rates in stochastic and dynamic queuing models of airport congestion. *Transportation Research Part E: Logistics and Transportation Review, 73*, 133-151. doi:http://dx.doi.org/10.1016/j.tre.2014.10.014.

Jacquillat, A., & Odoni, A. R. (2015b). An Integrated Scheduling and Operations Approach to Airport Congestion Mitigation. *Operations Research, 63*(6), 1390-1410. doi:10.1287/opre.2015.1428.

Jacquillat, A., Odoni, A. R., & Webster, M. D. (2016). Dynamic control of runway configurations and of arrival and departure service rates at JFK airport under stochastic queue conditions. *Transportation Science, 51*(1), 155-176.

Kafle, N., & Zou, B. (2016). Modeling flight delay propagation: A new analytical-econometric approach. *Transportation Research Part B: Methodological, 93*, 520-542. doi:http://dx.doi.org/10.1016/j.trb.2016.08.012.

Kergosien, Y., Gendreau, M., & Billaut, J.-C. (2017). A Benders decomposition-based heuristic for a production and outbound distribution scheduling problem with strict delivery constraints. *European Journal of Operational Research, 262*(1), 287-298.

Lee, C. K. M., Ng, K. K. H., Chan, H. K., Choy, K. L., Tai, W. C., & Choi, L. S. (2018). A multi-group analysis of social media engagement and loyalty constructs between full-service and low-cost carriers in Hong Kong. *Journal of Air Transport Management, 73*, 46-57. doi:https://doi.org/10.1016/j.jairtraman.2018.08.009.

Lee, C. K. M., Zhang, S., & Ng, K. K. (2019). Design of An Integration Model for Air Cargo Transportation Network Design and Flight Route Selection. *Sustainability, 11*(19), 5197.

Li, F., Chen, C.-H., Xu, G., Khoo, L. P., & Liu, Y. (2019a). Proactive mental fatigue detection of traffic control operators using bagged trees and gaze-bin analysis. *Advanced Engineering Informatics, 42*, 100987. doi:https://doi.org/10.1016/j.aei.2019.100987.

Li, F., Lee, C.-H., Chen, C.-H., & Khoo, L. P. (2019b). Hybrid data-driven vigilance model in traffic control center using eye-tracking data and context data. *Advanced Engineering Informatics, 42*, 100940. doi:https://doi.org/10.1016/j.aei.2019.100940.

Li, W., Xiao, M., Yi, Y., & Gao, L. (2019c). Maximum variation analysis based analytical target cascading for multidisciplinary robust design optimization under interval uncertainty. *Advanced Engineering Informatics, 40*, 81-92. doi:https://doi.org/10.1016/j.aei.2019.04.002.

Li, X., Yang, D., & Hu, M. (2018). A scenario-based stochastic programming approach for the product configuration problem under uncertainties and carbon emission regulations. *Transportation Research Part E: Logistics and Transportation Review, 115*, 126-146. doi:https://doi.org/10.1016/j.tre.2018.04.013.

Liang, Z., Xiao, F., Qian, X., Zhou, L., Jin, X., Lu, X., & Karichery, S. (2018). A column generation-based heuristic for aircraft recovery problem with airport capacity constraints and maintenance flexibility. *Transportation Research Part B: Methodological, 113*, 70-90. doi:https://doi.org/10.1016/j.trb.2018.05.007.

Liu, M., Zhang, F., Ma, Y., Pota, H. R., & Shen, W. (2016). Evacuation path optimization based on quantum ant colony algorithm. *Advanced Engineering Informatics, 30*(3), 259-267. doi:https://doi.org/10.1016/j.aei.2016.04.005.

Makui, A., Heydari, M., Aazami, A., & Dehghani, E. (2016). Accelerating Benders decomposition approach for robust aggregate production planning of products with a very limited expiration date. *Computers & Industrial Engineering, 100*, 34-51. doi:https://doi.org/10.1016/j.cie.2016.08.005.

Martins de Sá, E., Morabito, R., & de Camargo, R. S. (2018). Benders decomposition applied to a robust multiple allocation incomplete hub location problem. *Computers & Operations Research, 89*, 31-50. doi:https://doi.org/10.1016/j.cor.2017.08.001.

Montemanni, R., & Gambardella, L. M. (2005). The robust shortest path problem with interval data via Benders decomposition. *4OR, 3*(4), 315-328. doi:10.1007/s10288-005-0066-x.

Mulvey, J. M., Vanderbei, R. J., & Zenios, S. A. (1995). Robust optimization of large-scale systems. *Operations Research, 43*(2), 264-281.

Ng, K. K. H., & Lee, C. K. M. (2016a, 4-7 Dec. 2016). *Makespan minimization in aircraft landing problem under congested traffic situation using modified artificial bee colony algorithm.* Paper presented at the 2016 IEEE International Conference on Industrial Engineering and Engineering Management (IEEM), Bali, Indonesia.

Ng, K. K. H., & Lee, C. K. M. (2016b, 19-22 Sept. 2016). *A modified Variable Neighborhood Search for aircraft Landing Problem.* Paper presented at the 2016 IEEE International Conference on Management of Innovation and Technology (ICMIT), Bangkok, Thailand.

Ng, K. K. H., & Lee, C. K. M. (2017). *Aircraft Scheduling Considering Discrete Airborne Delay and Holding Pattern in the Near Terminal Area.* Paper presented at the Intelligent Computing Theories and Application: 13th International Conference, ICIC 2017, Liverpool, UK.

Ng, K. K. H., Lee, C. K. M., Chan, F. T. S., Chen, C.-H., & Qin, Y. (2020). A two-stage robust optimisation for terminal traffic flow problem. *Applied Soft Computing, 89*, 106048. doi:https://doi.org/10.1016/j.asoc.2019.106048.

Ng, K. K. H., Lee, C. K. M., Chan, F. T. S., & Lv, Y. (2018). Review on meta-heuristics approaches for airside operation research. *Applied Soft Computing, 66*, 104-133. doi:https://doi.org/10.1016/j.asoc.2018.02.013.

Ng, K. K. H., Lee, C. K. M., Chan, F. T. S., & Qin, Y. (2017a). Robust aircraft sequencing and scheduling problem with arrival/departure delay using the min-max regret approach. *Transportation Research Part E: Logistics and Transportation Review, 106*, 115-136. doi:https://doi.org/10.1016/j.tre.2017.08.006.

Ng, K. K. H., Lee, C. K. M., Zhang, S. Z., Wu, K., & Ho, W. (2017b). A multiple colonies artificial bee colony algorithm for a capacitated vehicle routing problem and re-routing strategies under time-dependent traffic congestion. *Computers & Industrial Engineering, 109*, 151-168. doi:https://doi.org/10.1016/j.cie.2017.05.004.

Ng, K. K. H., Tang, M. H. M., & Lee, C. K. M. (2015, 6-9 Dec. 2015). *Design and development of a performance evaluation system for the aircraft maintenance industry.* Paper presented at the 2015 IEEE International Conference on Industrial Engineering and Engineering Management (IEEM), Singapore, Singapore.

Pyrgiotis, N., Malone, K. M., & Odoni, A. (2013). Modelling delay propagation within an airport network. *Transportation Research Part C: Emerging Technologies, 27*, 60-75. doi:http://dx.doi.org/10.1016/j.trc.2011.05.017.

Qian, X., Mao, J., Chen, C.-H., Chen, S., & Yang, C. (2017). Coordinated multi-aircraft 4D trajectories planning considering buffer safety distance and fuel consumption optimization via pure-strategy game. *Transportation Research Part C: Emerging Technologies, 81*, 18-35. doi:https://doi.org/10.1016/j.trc.2017.05.008.

Saharidis, G. K. D., & Ierapetritou, M. G. (2010). Improving benders decomposition using maximum feasible subsystem (MFS) cut generation strategy. *Computers & Chemical Engineering, 34*(8), 1237-1245. doi:https://doi.org/10.1016/j.compchemeng.2009.10.002.

Samà, M., D'Ariano, A., Corman, F., & Pacciarelli, D. (2017a). Metaheuristics for efficient aircraft scheduling and re-routing at busy terminal control areas. *Transportation Research Part C: Emerging Technologies, 80*, 485-511. doi:https://doi.org/10.1016/j.trc.2016.08.012.

Samà, M., D'Ariano, A., D'Ariano, P., & Pacciarelli, D. (2014). Optimal aircraft scheduling and routing at a terminal control area during disturbances. *Transportation Research Part C: Emerging Technologies, 47*, 61-85. doi:http://dx.doi.org/10.1016/j.trc.2014.08.005.

Samà, M., D'Ariano, A., D'Ariano, P., & Pacciarelli, D. (2015). Air traffic optimization models for aircraft delay and travel time minimization in terminal control areas. *Public Transport, 7*(3), 321-337. doi:10.1007/s12469-015-0103-x.

Samà, M., D'Ariano, A., D'Ariano, P., & Pacciarelli, D. (2017b). Scheduling models for optimal aircraft traffic control at busy airports: Tardiness, priorities, equity and violations considerations. *Omega, 67*, 81-98. doi:https://doi.org/10.1016/j.omega.2016.04.003.

Siddiqui, S., Azarm, S., & Gabriel, S. (2011). A modified Benders decomposition method for efficient robust optimization under interval uncertainty. *Structural and Multidisciplinary Optimization, 44*(2), 259-275. doi:10.1007/s00158-011-0631-1.

Wang, Y., Zhang, Y., & Tang, J. (2019). A distributionally robust optimization approach for surgery block allocation. *European Journal of Operational Research, 273*(2), 740-753. doi:https://doi.org/10.1016/j.ejor.2018.08.037.

Wee, H. J., Lye, S. W., & Pinheiro, J.-P. (2018). A Spatial, Temporal Complexity Metric for Tactical Air Traffic Control. *The Journal of Navigation*, 1-15.

Wee, H. J., Lye, S. W., & Pinheiro, J.-P. (2019). An integrated highly synchronous, high resolution, real time eye tracking system for dynamic flight movement. *Advanced Engineering Informatics, 41*, 100919. doi:https://doi.org/10.1016/j.aei.2019.100919.

Wu, C.-L., & Law, K. (2019). Modelling the delay propagation effects of multiple resource connections in an airline network using a Bayesian network model. *Transportation Research Part E: Logistics and Transportation Review, 122*, 62-77. doi:https://doi.org/10.1016/j.tre.2018.11.004.

Xu, X., Cui, W., Lin, J., & Qian, Y. (2013). Robust makespan minimisation in identical parallel machine scheduling problem with interval data. *International Journal of Production Research, 51*(12), 3532-3548. doi:10.1080/00207543.2012.751510.

Yang, J., Tang, D., Li, S., Wang, Q., & Zhu, H. (2020). An improved iterative stochastic multi-objective acceptability analysis method for robust alternative selection in new product development. *Advanced Engineering Informatics, 43*, 101038. doi:https://doi.org/10.1016/j.aei.2020.101038.

Zarrinpoor, N., Fallahnezhad, M. S., & Pishvaee, M. S. (2018). The design of a reliable and robust hierarchical health service network using an accelerated Benders decomposition algorithm. *European Journal of Operational Research, 265*(3), 1013-1032. doi:https://doi.org/10.1016/j.ejor.2017.08.023.

Zou, B., & Hansen, M. (2012). Impact of operational performance on air carrier cost structure: Evidence from US airlines. *Transportation Research Part E: Logistics and Transportation Review, 48*(5), 1032-1048. doi:http://dx.doi.org/10.1016/j.tre.2012.03.006.